

Original Article

Cite this article: Śliwińska KK, Jelby ME, Grundvåg S-A, Nøhr-Hansen H, Alsen P, and Olausen S (2020) Dinocyst stratigraphy of the Valanginian–Aptian Rurikfjellet and Helvetiafjellet formations on Spitsbergen, Arctic Norway. *Geological Magazine* **157**: 1693–1714. <https://doi.org/10.1017/S0016756819001249>

Received: 18 May 2019

Revised: 4 September 2019

Accepted: 9 September 2019

First published online: 11 February 2020





Keywords:

dinocysts; biostratigraphy; Lower Cretaceous; Spitsbergen; Arctic

Author for correspondence:

Kasia K. Śliwińska, Email: kksl@geus.dk

Dinocyst stratigraphy of the Valanginian–Aptian Rurikfjellet and Helvetiafjellet formations on Spitsbergen, Arctic Norway

Kasia K. Śliwińska¹ , Mads E. Jelby² , Sten-Andreas Grundvåg³,
Henrik Nøhr-Hansen¹ , Peter Alsen¹  and Snorre Olausen⁴

¹Department of Stratigraphy, Geological Survey of Denmark and Greenland (GEUS), Øster Voldgade 10, DK-1350 Copenhagen K, Denmark; ²Department of Geosciences and Natural Resource Management, University of Copenhagen, Øster Voldgade 10, DK-1350 Copenhagen K, Denmark; ³Department of Geosciences, UiT The Arctic University of Norway, P.O. Box 6050, Langnes, N-9037 Tromsø, Norway and ⁴Department of Arctic Geology, The University Centre in Svalbard (UNIS), P.O. Box 156, N-9171 Longyearbyen, Norway

Abstract

In order to improve the understanding of how the high northern latitudes responded to the escalating warming which led to the middle Cretaceous super greenhouse climate, more temperature proxy records from the High Arctic are needed. One of the current obstacles in obtaining such records is poor age control on the Lower Cretaceous strata in the Boreal region. Here, we provide a biostratigraphic framework for the Rurikfjellet and Helvetiafjellet formations representing the lower part of the Lower Cretaceous succession on Spitsbergen. We also attempt to date the boundary between the Agardhfjellet and the Rurikfjellet formations. This study is based on dinoflagellate cysts (dinocysts) from three onshore cores (DH1, DH2 and DH5R) and three outcrop sections (Bohemianflya, Myklegardfjellet and Ullaberget). Relatively abundant and well-preserved dinocyst assemblages from the Rurikfjellet Formation date this unit as early Valanginian – early Barremian. The dinocyst assemblages from the Helvetiafjellet Formation are significantly impoverished and are characterized by reworking, but collectively indicate a Barremian–Aptian age for this formation.

1. Introduction

The Early Cretaceous period (~145–100.5 Ma; Ogg *et al.* 2016) was characterized by major tectonic activity, climatic changes and global perturbations in the carbon cycle (e.g. Huber *et al.* 2018). The break-up of the supercontinent Pangaea, which terminated around 175 Ma (e.g. Holden, 1970; Rogers & Santosh, 2004), led to the formation of two minor supercontinents: Laurasia to the north, and Gondwana to the south separated by the newly formed Tethys Ocean. The Barents Sea Shelf including Svalbard (palaeolatitude 60° N at 140 Ma; calculated after van Hinsbergen *et al.* 2015), Arctic Canada, Greenland and northern Russia were located on the northern flank of Laurasia as part of the large circum-Arctic, relatively cold Boreal Realm (Scotese, 2014). In the Tethys Ocean to the south, warm to tropical water conditions prevailed, leading to a bloom of calcareous nannoplankton and foraminifera. The Tethys and Boreal seas were connected by a shallow, narrow seaway between Greenland and Baltica. The seaway formed in response to rifting during the initial stage of the formation of the North Atlantic Ocean at that time (e.g. Gradstein *et al.* 1999). The palaeogeographical configuration in the Early Cretaceous favoured a diversification of marine organisms and diachroneity of ammonite bio-events, which traditionally constitute the primary tool for Cretaceous biostratigraphy (e.g. Lehmann, 2015). This has led to the creation of two separate biozonation schemes: one for the Boreal and one for the Tethyan Realm. Both are still applicable across the Jurassic–Cretaceous transition (Ogg *et al.* 2012).

Temperature proxy data from Early Cretaceous high latitudes are limited (Ditchfield, 1997; Littler *et al.* 2011; Jenkyns *et al.* 2012; Price & Passey, 2013), but it is assumed that the global climate was generally warm and humid with low latitudinal temperature gradients (e.g. O'Brien *et al.* 2017). In contrast, some studies suggest that the polar regions during the Early Cretaceous were rather cold (e.g. De Lurio & Frakes, 1999; Smelror *et al.* 2009). Increased volcanic activity (including oceanic crust formation, formation of large igneous provinces and subduction-related arc volcanism) (e.g. Johnston *et al.* 2011; Koopmann *et al.* 2014; Polteau *et al.* 2016) forced an increased concentration of atmospheric greenhouse gases (methane and CO₂), and led to a gradual global warming (e.g. Huber *et al.* 2018). A climatic maximum of this extreme global warmth, the so-called Cretaceous Hot Greenhouse climate, was reached between 95 and 80 Ma (Huber *et al.* 2018). During the

Cretaceous Period a number of oceanic anoxic events (OAEs) led to the deposition of organic carbon-rich sediments (Leckie *et al.* 2002; Trabucho Alexandre *et al.* 2010). At least four of these events took place during the Early Cretaceous: the OAE1a, OAE1b, OAE1c and OAE1d (Erbacher *et al.* 1996). The most widely recognized is the OAE1a, which occurred during the earliest Aptian (Leckie *et al.* 2002; Jenkyns, 2010; Herrle *et al.* 2015; Midtkandal *et al.* 2016). The characteristic stable carbon isotope ($\delta^{13}\text{C}$) excursions related to OAEs can be used for the correlation of carbon isotope records (Herrle *et al.* 2015; Midtkandal *et al.* 2016; Vickers *et al.* 2016). However, while the climatic history of the Tethys (e.g. Hochuli *et al.* 1999; Bottini *et al.* 2015; Bottini & Erba, 2018) and the European Boreal Realm (e.g. Mutterlose *et al.* 2009) are relatively well studied, the climate of the Early Cretaceous Arctic is relatively less understood. Many of the published palaeotemperature records contradict evidence for both warm and cool periods (e.g. Galloway *et al.* 2015; Hurum *et al.* 2016a; discussion in Vickers *et al.* 2016). Some of the contradictions may be owing to limited temperature data from the High Arctic and the lack of a concise biostratigraphic framework for the Cretaceous strata in this region.

On Spitsbergen (Svalbard, Arctic Norway) the Lower Cretaceous succession is divided into three formations: the Rurikfjellet, Helvetiafjellet and Carolinefjellet formations. The first biostratigraphic study of the Rurikfjellet Formation was based on macrofossils (bivalves and ammonites), and dated the formation as Berriasian – upper Hauterivian (for references see Grøsfjeld, 1991). The first dinocyst-based study of the Lower Cretaceous succession on Spitsbergen was provided by Bjærke & Thusu (1976). The first comprehensive study of Lower Cretaceous dinocysts on Spitsbergen was carried out by Bjærke (1978), who observed that the dinocyst assemblages of the Berriasian, Valanginian and Hauterivian are similar to assemblages from NW Europe and Arctic Canada.

The aim of this paper is to provide a concise age model for the Lower Cretaceous Rurikfjellet and Helvetiafjellet formations on Spitsbergen. The study is primarily based on dinocysts from six onshore outcrop and sediment core sections. The new data are discussed in the context of existing literature dealing with the palynology of the Arctic and the European Boreal Province.

2. Regional setting

Spitsbergen is the largest island in the Svalbard archipelago, and is located today at *c.* 76–80° N. The Svalbard archipelago represents the uplifted and exposed northwestern corner of the Barents Sea Shelf. The Barents Sea Shelf is bounded to the west by the Western Barents Sea Margin, and to the south and east by the Baltic Shield and Novaya Zemlya archipelago (e.g. Henriksen *et al.* 2011). During the Early Cretaceous, the Svalbard platform was part of a shallow, epicontinental sag basin (e.g. Henriksen *et al.* 2011) on the northern margin of Pangaea (Torsvik *et al.* 2002). The Lower Cretaceous succession in Svalbard is over 1000 m thick and exhibits a large-scale regressive–transgressive stacking pattern. This depositional cycle was controlled by regional thermo-tectonic uplift in the north, followed by subsequent quiescence and subsidence (Gjelberg & Steel, 1995; Midtkandal *et al.* 2007; Midtkandal & Nystuen, 2009). The magmatic activity in Svalbard and the surrounding areas related to the emplacement of the High Arctic Large Igneous Province (HALIP) peaked in

Barremian to the early Aptian (Corfu *et al.* 2013; Senger *et al.* 2014; Polteau *et al.* 2016). An early Barremian uplift and associated southward tilting of the shelf caused the formation of a regionally extensive subaerial unconformity, which now forms the boundary between the Rurikfjellet and Helvetiafjellet formations (e.g. Gjelberg & Steel, 1995; Midtkandal & Nystuen, 2009; Grundvåg *et al.* 2017). This event was followed by a transgression related to a long-term relative global sea-level rise (Gjelberg & Steel, 1995; Midtkandal & Nystuen, 2009). In the Late Cretaceous, subaerial exposure of Svalbard resulted in a major hiatus spanning the entire Upper Cretaceous (Harland, 1997; Dörr *et al.* 2012).

3. Lower Cretaceous lithostratigraphy of Spitsbergen

The Lower Cretaceous succession on Spitsbergen is subdivided into the Rurikfjellet, Helvetiafjellet and Carolinefjellet formations. The succession forms the upper part of the Adventdalen Group (which also includes the Upper Jurassic Agardhfjellet Formation; Parker, 1967), and is primarily exposed along the margins of the Central Tertiary Basin. The Rurikfjellet Formation consists of a lower offshore shale-dominated succession (the Wimanfjellet Member), which is overlain by a storm-dominated shallow-marine succession (the Kikutodden Member) of interbedded shale, siltstone and sandstone (Fig. 1). The Rurikfjellet Formation unconformably overlies the Upper Jurassic – lowermost Cretaceous Agardhfjellet Formation (Dypvik *et al.* 1991), and its base is marked either by (i) a condensed glauconitic clay unit (the Myklegardfjellet Bed; Dypvik *et al.* 1991, 1992); (ii) a highly tectonized decollement zone; or (iii) by an abrupt change in the macrofossil fauna. In the central part of Spitsbergen, the Wimanfjellet Member is intersected by a thick succession of gravity flow deposits informally defined as the Adventpynten member (Grundvåg *et al.* 2017). The Kikutodden Member represents prodeltaic to shallow-marine deposits which were sourced from the northwest and exhibit progradation towards the southeast (Fig. 1; Dypvik *et al.* 1991). The overall changes in the lithologies of the Rurikfjellet Formation reflect the shallowing development of the basin as a response to uplift in the north.

The boundary between the Rurikfjellet and Helvetiafjellet formations is marked by a regionally extensive subaerial unconformity (e.g. Midtkandal & Nystuen, 2009; Grundvåg *et al.* 2017). The Helvetiafjellet Formation represents a fluvio-deltaic to paralic depositional system reflecting long-term relative sea-level rise (Gjelberg & Steel, 1995; Midtkandal & Nystuen, 2009). The Helvetiafjellet Formation represents the most proximally deposited strata within the Lower Cretaceous succession on Spitsbergen. The Helvetiafjellet Formation is overlain by storm-dominated open marine shelf deposits of the Carolinefjellet Formation (Gjelberg & Steel, 1995; Grundvåg *et al.* 2017) (Fig. 1).

4. Previous studies of Lower Cretaceous boreal dinocyst assemblages

Dinocyst studies of Arctic Lower Cretaceous successions are relatively rare and scattered across the Canadian Arctic (Pocock, 1976; Brideaux, 1977; McIntyre & Brideaux, 1980; Davies, 1983; Nøhr-Hansen & McIntyre, 1998), Greenland (Nøhr-Hansen 1993; Pedersen & Nøhr-Hansen, 2014; Piasecki *et al.* 2018;

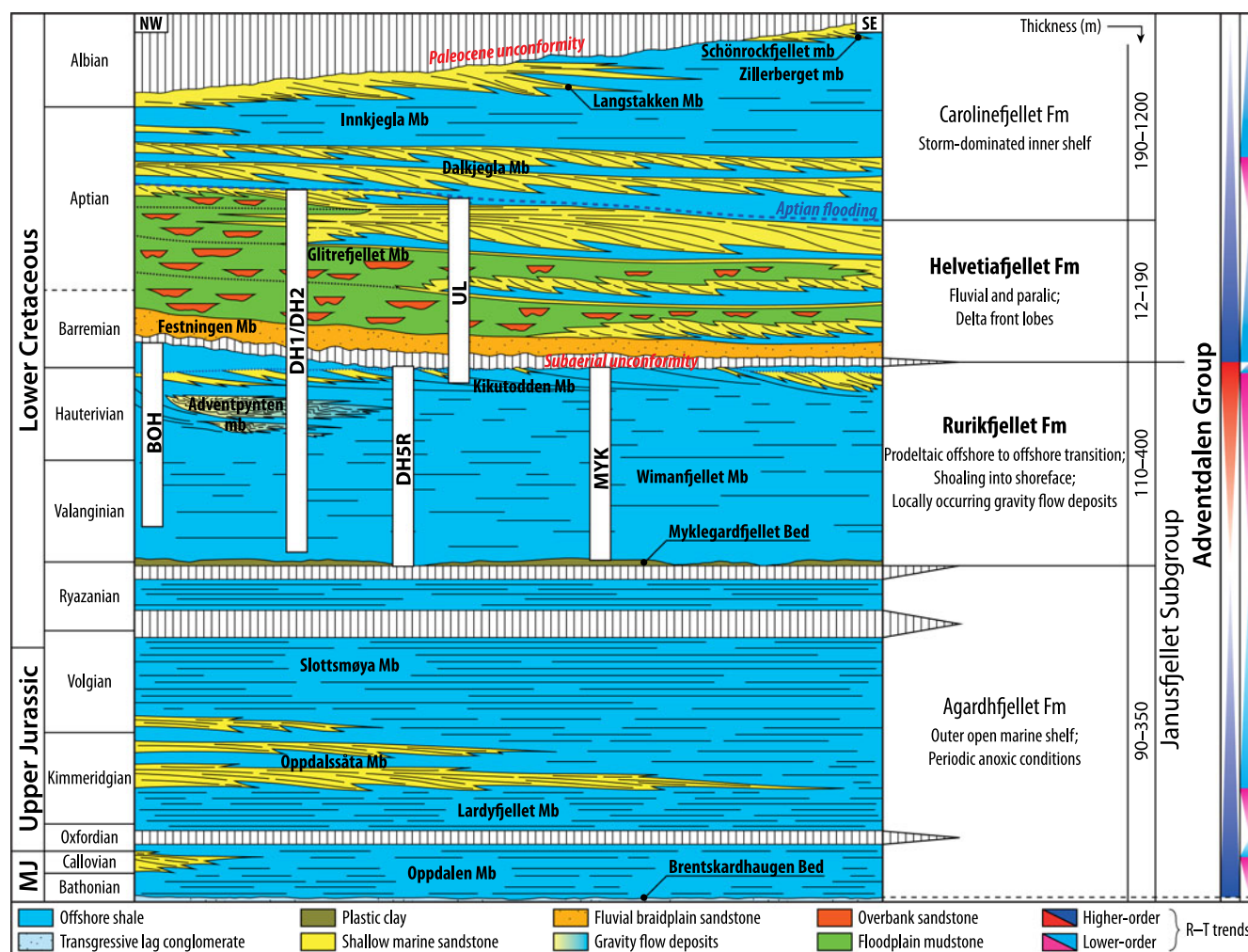


Fig. 1. Stratigraphic cross-section showing the regional development of the Upper Jurassic to Lower Cretaceous Adventdalen Group on Spitsbergen. Modified after Alsen *et al.* (2019). White bars show the time span for each of the studied sites: three onshore cores DH1, DH2, DH5R; and three outcrop sections: Bohemanflya (BOH), Ullaberget (UL) and Myklegardfjellet (MYK).

Nøhr-Hansen *et al.* 2019), the Barents Sea (Århus *et al.* 1990; Smelror *et al.* 1998; Smelror & Dypvik, 2005; Smelror & Dypvik, 2006; Kairanov *et al.* 2018), Arctic Norway (Løfaldi & Thusu, 1976; Bjærke, 1978; Thusu, 1978; Århus *et al.* 1986, 1990; Århus, 1991; Grøsfjeld, 1991; Hurum *et al.* 2016b; Smelror & Larssen, 2016; Smelror *et al.* 2018; Hammer *et al.* 2018; Rakociński *et al.* 2018; Grundvåg *et al.* 2019) and Arctic Russia (Smelror, 1986; Lebedeva & Nikitenko, 1999; Riding *et al.* 1999; Pestchevitskaya, 2007; Nikitenko *et al.* 2008; Pestchevitskaya *et al.* 2011). Some early Canadian studies provided dinocyst zonation (e.g. Pocock, 1976; Davey, 1982; Davies, 1983), but the diversity of the studied material was limited, and ranges of specific taxa were poorly constrained compared to the more recent and robust dinocyst zonation established for NE Greenland (Nøhr-Hansen, 1993; Nøhr-Hansen *et al.* 2019). A number of dinocyst studies from the North Sea Basin and NW Europe, often referred to as the European Boreal Province, provide well-constrained zonation schemes (Davey, 1979a, 1982; Heilmann-Clausen, 1987; Costa & Davey, 1992; Duxbury, 2001; Bailey, 2019).

The first chronostratigraphic framework for the Rurikfjellet Formation (at that time known as the Rurikfjellet Member) was based on ammonites and bivalves (for references see Grøsfjeld, 1991). An informally defined Lower Cretaceous palynological

zonation of Spitsbergen was introduced in a confidential report by Århus (1988). Low dinocyst abundances and low diversities have been reported from studies of the Lower Cretaceous succession on Spitsbergen and in the Barents Sea (e.g. Århus *et al.* 1990; Århus, 1992). The dinocysts of the Rurikfjellet Formation have been investigated in less than a dozen peer-reviewed publications. Notable works include Bjærke & Thusu (1976), Bjærke (1978), Århus *et al.* (1990), Århus (1991, 1992), Grøsfjeld (1991), and more recently Midtkandal *et al.* (2016) and Grundvåg *et al.* (2017). The palynology of the Helvetiafjellet Formation has been studied to an even lesser extent (Grøsfjeld, 1991; Midtkandal *et al.* 2016). A number of recent studies on the seismic stratigraphy of the Lower Cretaceous succession in the southwestern Barents Sea provide an updated preliminary age model based on dinocysts (Marin *et al.* 2017; Kairanov *et al.* 2018; Marin *et al.* 2018a,b).

5. Studied sections

5.a. The Bohemanflya outcrop section

The Bohemanflya outcrop section (78° 24' 32.6" N, 14° 41' 18.9" E) is the northernmost locality investigated in this study, exposing Lower Cretaceous strata in central Spitsbergen (Fig. 2). At this

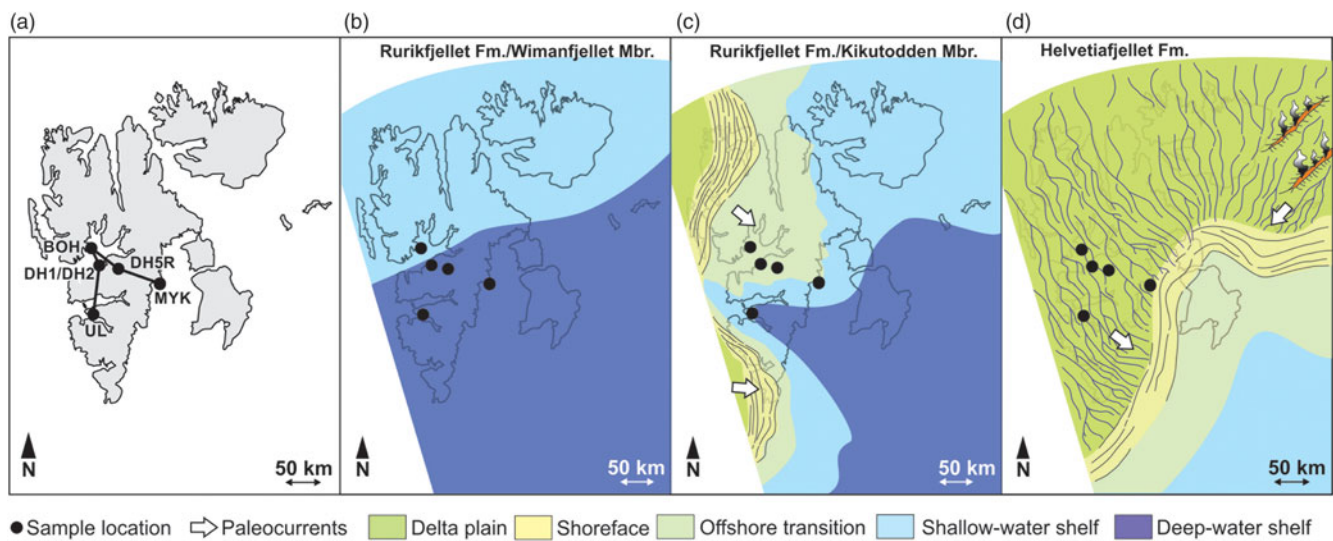


Fig. 2. (a) Black dots mark the positions of the studied sites: BOH – Bohemanflya; UL – Ullaberget; Myk – Myklegardfjellet outcrop sections as well as DH1, DH2 and DH5R onshore cores. Palaeogeography of Spitsbergen from the Valanginian to early Aptian (after Grundvåg & Olausson, 2017; Grundvåg *et al.* 2017). (b) Palaeogeography during the deposition of the Wimanfjellet Member. (c) Palaeogeography during the deposition of the Kikutodden Member. (d) Palaeogeography during the earliest Barremian deposition of the Helvetiafjellet Formation (the Festningen Member).

locality, the Wimanfjellet Member constitutes a measurable thickness of *c.* 45 m and consists of generally black shale with scattered siderite concretions and nodules or stratabound siderite layers. In certain intervals, the Wimanfjellet Member is tectonically disturbed. The overlying Kikutodden Member (Fig. 1) is *c.* 83 m thick, and is siltstone and sandstone dominated. The upper part of the succession exhibits gravel-rich hummocky cross-stratified sandstone, which is occasionally truncated by the subaerial unconformity constituting the base of the overlying Festningen Member of the Helvetiafjellet Formation. In this study, we collected samples from across the entire exposed length of the Rurikfjellet Formation (*~*130 m; online Supplementary Material Fig. S1). The sedimentological profile of the outcrop is provided in Grundvåg *et al.* (2019) and Jelby *et al.* (2020).

5.b. The Myklegardfjellet outcrop section

The Myklegardfjellet outcrop section (78° 03' 18.8" N, 18° 42' 15.4" E) is the easternmost locality investigated in this study, exposing Upper Jurassic – Lower Cretaceous strata at the northeastern side of Agardhbukta, east coast of Spitsbergen (Fig. 2). At this locality, the Rurikfjellet Formation is entirely composed of homogeneous shale of the Wimanfjellet Member (Fig. 1), reaching a thickness of 166 m. The shale is characterized by absent to low degrees of bioturbation as well as scattered siderite concretions, nodules and fossiliferous stratabound siderite layers with abundant bivalves. The Kikutodden Member is either not preserved in this locality, or it is covered by scree. This outcrop section is the type locality of the Myklegardfjellet Bed (Birkenmajer *et al.* 1979; Dypvik *et al.* 1992), demarcating the base of the Rurikfjellet Formation by a well-exposed *c.* 3 m thick unit of glauconitic, plastic clays. The Rurikfjellet Formation is unconformably overlain by sandstones of the Festningen Member of the overlying Helvetiafjellet Formation. In this study we investigate *c.* 130 m of deposits from the Wimanfjellet Member (online Supplementary Material Fig. S2). The sedimentological profile of the outcrop is provided in Grundvåg *et al.* (2019) (<https://dx.doi.org/10.17850/njg006>).

5.c. The Ullaberget outcrop section

The Ullaberget outcrop section (77° 37' 04.2" N 15° 11' 17.9" E) is the southernmost locality investigated in this study, exposing Lower Cretaceous strata at the northwestern side of Van Keulenfjorden. At this locality, the Rurikfjellet Formation is *c.* 200 m thick (the base is not exposed) and dominated by homogeneous shale of the Wimanfjellet Member. For the purpose of this study, only three samples from the uppermost 2 m of the Rurikfjellet Formation were collected (online Supplementary Material Fig. S3). The shale is characterized by a lack of or low degree of bioturbation. Siderite concretions, nodules and fossiliferous stratabound layers occur. Thin- and lenticular-bedded sandstone occurs sporadically in the upper part of the unit, representing the distal part of the Kikutodden Member. The Rurikfjellet Formation is unconformably overlain by sandstones of the Helvetiafjellet Formation (Midtkandal *et al.* 2008). The remaining part of the Helvetiafjellet Formation displays a transgressive development, comprising various paralic deposits, including tidal channel fills, and coarsening-upwards bay fill sequences (Gjelberg & Steel, 1995; Midtkandal & Nystuen, 2009), which lithostratigraphically belong to the Glitrefjellet Member. At this locality, the Helvetiafjellet Formation is conformably overlain by a 20–30 m thick shale unit of the Carolinefjellet Formation.

5.d. The DH1 and DH2 cores

The DH1 (78° 23' 60.8" N, 15° 54' 57.6" E) and DH2 (78° 23' 59.9" N, 15° 54' 68.4" E) cores were drilled *c.* 3 km to the northwest of Longyearbyen close to the airport, in relation to CO₂ sequestration studies (Braathen *et al.* 2012). The cores span the Rurikfjellet and Helvetiafjellet formations, and the lower part of the Carolinefjellet Formation (Fig. 1). In these wells, the Rurikfjellet Formation is *c.* 225 m thick (*~*440–215 m) and conformably overlies shale of the Agardhfjellet Formation (e.g. Grundvåg *et al.* 2017). The boundary between the two units is tectonically disturbed, representing a decollement zone that formed during the Palaeogene shortening (Dietmar Müller & Spielhagen, 1990). The lower part of the Rurikfjellet

Formation consists of a ~140 m thick succession of gravity flow deposits of the Adventpynten member. The upper part of the Rurikfjellet Formation consists of a 30–40 m thick mudstone-dominated unit which grades upwards into the sandstone-dominated Kikutodden Member. The Rurikfjellet Formation is unconformably overlain by a 12 m thick sandstone unit representing the Festningen Member of the Helvetiafjellet Formation (Grundvåg *et al.* 2017). The upper c. 60 m of the Helvetiafjellet Formation consists of interbedded sandstone, shale and thin coal layers of the Glitrefjellet Member, representing various alluvial to paralic depositional environments. The thicknesses of all lithostratigraphic units across the investigated interval in the two cores are shown in online Supplementary Material Figure S4 (DH1) and online Supplementary Material Figure S5 (DH2). The Helvetiafjellet Formation is unconformably overlain by a ~10 m thick shale unit of the overlying Dalkjegla Member of the Carolinefjellet Formation. The sedimentological profile of both cores are provided in Grundvåg *et al.* (2019) (<https://dx.doi.org/10.17850/njg006>).

5.e. The DH5R core

The DH5R core (78° 12' 13.1" N 15° 49' 08.6" E) was drilled c. 4 km to the southeast of Longyearbyen in central Spitsbergen, also in relation to CO₂ sequestration studies (Braathen *et al.* 2012). The studied part of the core spans from the uppermost Agardhfjellet Formation to the Carolinefjellet Formation. The Rurikfjellet Formation is c. 230 m thick (410–180 m) and overlies shale of the Agardhfjellet Formation (Koevoets *et al.* 2018). The lithology of the Rurikfjellet Formation differs from that observed in the DH1 and DH2 cores. In the DH5R core, the formation displays homogeneous to sparsely bioturbated shale with scattered siderite concretions and bivalves of the Wimanfjellet Member, which coarsen into silty shale, heavily bioturbated siltstone and hummocky cross-stratified sandstone of the overlying Kikutodden Member. The Helvetiafjellet (180–120 m) and Carolinefjellet formations display the same stratigraphic development as in the DH1 and DH2 cores. The sedimentological profile of the core is provided in Grundvåg *et al.* (2019) (<https://dx.doi.org/10.17850/njg006>).

6. Analytical methods

Sediment samples for palynological analysis were collected during fieldwork and core logging campaigns in 2013 to 2016. A total of 82 samples were collected, with 40 samples from Bohemanflya, Myklegardfjellet and Ullaberget, and 42 samples from the DH1, DH2 and DH5R cores. The majority of samples were collected from the Rurikfjellet Formation, including 8 samples from DH1, 14 samples from DH2, 15 samples from DH5R, 12 samples from Bohemanflya, 13 samples from Myklegardfjellet and 3 samples from Ullaberget. The Helvetiafjellet Formation was sampled only in the DH2 core (3 samples) and Ullaberget outcrop section (12 samples). Furthermore, in order to improve the age of the base of the Lower Cretaceous succession in our study area, we have analysed three samples from the upper part of the Agardhfjellet Formation from the DH5R core (at 458.0, 440.0 and 410.0 m).

Preparation of palynological slides was performed at the Geological Survey of Denmark and Greenland (GEUS). Between 20 and 45 g of sediment were dried in an oven for 24 hours at 30 °C and manually ground. Hydrochloric (HCl; 3.5 % and

18 %) and hydrofluoric (HF; 40 %) acids were used for dissolving carbonates and silicates, respectively. After each step, samples were neutralized with 0.5 % citric acid (C₆H₈O₇) at 70 °C. The organic residuum from each sample was filtered using an 11 µm nylon mesh, and a first (kerogen) slide was prepared. Subsequently, the residua were oxidized with HNO₃ for 8 min in order to remove amorphous kerogen particles. Samples with high concentrations of amorphous kerogen particles were oxidized for additional 1 to 5 min. After each oxidation step, residua were washed with a weak solution (5 %) of potassium hydroxide (KOH), and a fraction of the residue was taken for palynological slide preparation. Some of the residua were additionally briefly submerged in a boiling mixture of HNO₃:KOH (1:1), and filtered using a 21 µm nylon mesh. The high concentration of coal and wood particles present in some of the samples was removed by swirling, and minerals were removed by heavy liquid separation (ZnBr; density 2.3 g/mL). After each of these steps, organic residua were filtered using a 21 µm nylon mesh. To concentrate palynomorphs, organic residua from some of the samples were filtered using a 30 µm nylon mesh. All palynological slides and (if available) organic residua are stored at GEUS.

The palynological slides were analysed using a transmitted light microscope. When possible, a minimum of 300 dinocysts were counted in a single slide. In a few cases, when a single slide contained less than 300 dinocysts, it was necessary to count one or two additional slides. The dinocyst taxonomy follows Williams *et al.* (2017). All dinocysts recorded in this study are listed in Table 1. Selected dinocysts are presented in Figures 3–6. Coordinates of the photographed specimens are given following the method described by Śliwińska (2019).

7. Results and discussion

Two out of three samples from the Agardhfjellet Formation were barren with respect to dinocysts. Virtually all analysed samples from the Rurikfjellet Formation and the Helvetiafjellet Formation yielded dinocysts. The diversity, abundance and preservation are highly variable spatially and temporally. In samples where dinocysts were rare or absent, the assemblages are dominated by black and dark brown wood particles, as well as pollen grains.

In some levels, despite counting more than one palynological slide, there were less than 300 dinocysts in total (e.g. in the uppermost samples of the DH5R core). The dinocyst assemblages were particularly impoverished in the Ullaberget outcrop section, and in the DH1 and DH2 cores. In comparison, the dinocyst assemblages of the Myklegardfjellet outcrop section show the highest richness of species (online Supplementary Material Fig. S2).

Within the Rurikfjellet Formation we distinguish several age-diagnostic dinocysts: *Endoscrinium hauerivianum* (Fig. 3o, p; Appendix 1a), *Gochteodinia villosa* subsp. *villosa* (Fig. 4b; Appendix 1b), *Muderongia australis* (Fig. 4e; Appendix 1c), *Muderongia tetracantha* (Fig. 4d; Appendix 1d), *Nelchinopsis kostromiensis* (Fig. 4m, n; Appendix 1e), *Oligosphaeridium complex* (Fig. 5h; Appendix 1h), *Palaecysta palmula* (Fig. 5k; Appendix 1i), *Subtilisphaera perlucida* (Fig. 6g; Appendix 1l) and *Tubotuberella apatela* (Fig. 6i–k; Appendix 1m). Other typical dinocysts observed within the formation include *Cyclonephelium cuculliforme sensu Århus, 1990* (Fig. 5l), *Discorsia nannus* (Fig. 3m), *Dissiliodinium acmeum* (Fig. 3k), *Nyktericysta? pannosa* (Fig. 4o, p), *Oligosphaeridium abaculum* (Fig. 5f; Appendix 1g), *Phoberocysta neocomica* (Fig. 5c), *Pseudoceratium pelliferum* (Fig. 5j),

Table 1. List of palynomorphs recorded in this study including a reference to photographs (Figs 3–6) and range charts (online Supplementary Material Figs S1–S6)

Palynomorph name in alphabetical order according to genus then species	Photo	Fig. S1	Fig. S2	Fig. S3	Fig. S4	Fig. S5	Fig. S6
<i>Apteodinium spongiosum</i>	3b–e		35		5		21
<i>Apteodinium</i> spp.				1			28
<i>Athigmatocysta glabra</i>							33
<i>Atopodinium haromense</i>	3f	37	58	34			
<i>Bourkidinium granulatum</i>			33				
<i>Bourkidinium</i> spp.				32			
<i>Canningia reticulata</i>				23			
<i>Cassiculosphaeridia magna</i>							10
<i>Chlamydophorella nyei</i>				27	18		
<i>Chlamydophorella</i> spp.				2			
<i>Circulodinium</i> aff. <i>attadalicum</i> sensu Nøhr-Hansen, 1993				28		33	
<i>Circulodinium distinctum</i>	3g–j	42	15	35	8	19	25
<i>Circulodinium</i> sp. 1			32				
<i>Circulodinium</i> spp.		8	36	12	19	26	31
<i>Cleistosphaeridium</i> spp.			44				37
<i>Cribroperidinium</i> sp. 1			6	31			
<i>Cribroperidinium</i> spp.		9	12		6	14	4
<i>Cyclonephelium cuculliforme</i> sensu Århus, 1990	5l		10				
<i>Dingodinium cerviculum</i>	3n	5	37	7	14	9	16
<i>Discorsia nannus</i>	3m	27	34				47
<i>Dissiliodinium acmeum</i>	3k		8				
<i>Downiesphaeridium?</i> <i>aciculare</i>		45	64		23	27	54
<i>Endoscrinium hauerivianum</i>	3o, p	22	56	39	33	13, 38	36
<i>Endoscrinium</i> sp. 1	3l	1	51		1	3	29
<i>Endoscrinium</i> spp.				38			
? <i>Escharisphaeridia rudis</i>	5b		27				32
<i>Florentinia</i> spp.				3			
<i>Gardodinium trabeculosum</i>		43	65				
<i>Gochteodinia judilentiniae</i>			25				
<i>Gochteodinia villosa</i> subsp. <i>multifurcata</i>	4a, c		28		2		12
<i>Gochteodinia villosa</i>	4b		29			39	11
<i>Gonyaulacysta</i> sp. 1			41				
<i>Gonyaulacysta</i> spp.		25	16	30			14
<i>Heslertonia heslertonensis</i>		30	31				
<i>Hystrichodinium voigtii</i>		35	22				46
<i>Hystrichosphaeridium arborispinum</i>							49
<i>Isthmocystis distincta</i>	4i		23				
<i>Kiokansium unituberculatum</i>	4k	19	38		35		42
<i>Kleithriasphaeridium eoinodes</i>	4j		55				
<i>Lagenorhysis delicatula</i>							22
<i>Leptodinium</i> spp.		21					
<i>Meiouragonyaulax stoveri</i>	4l	33	43				35
<i>Muderongia asymmetrica</i>							55

(Continued)

Table 1. (Continued)

Palynomorph name in alphabetical order according to genus then species	Photo	Fig. S1	Fig. S2	Fig. S3	Fig. S4	Fig. S5	Fig. S6
<i>Muderongia australis</i>	4e	40	62	40	30	15	43
<i>Muderongia extensiva</i>	4h	39					
<i>Muderongia parvata</i>						36	52
<i>Muderongia simplex</i>	4f		46				44
<i>Muderongia simplex</i> subsp. <i>microperforata</i> sensu Nøhr-Hansen, 1993							56
<i>Muderongia</i> spp.		10	50	24	9	17	45
<i>Muderongia tetracantha</i>	4d	36	61	10	22		40
<i>Muderongia tetracantha/extensiva</i>	4g	31	59		28		41
<i>Nelchinopsis kostromiensis</i>	4m, n	6	39	4, 41	27	10	18
<i>Nyktericysta?</i> aff. <i>pannosa</i>	4o, p	41			20		
<i>Nyktericysta vitrea</i>						34	
<i>Nyktericysta</i> spp.							57
<i>Odontochitina nuda</i>	5e			36		30	
<i>Odontochitina</i> spp.				26			
<i>Oligosphaeridium albertense</i>				22			
<i>Oligosphaeridium abaculum</i>	5f	11	53		7	22	34
<i>Oligosphaeridium asterigerum</i>	5i	12	24	13	12	1	26
<i>Oligosphaeridium complex</i>	5h	13	17	18	15	4	19
<i>Oligosphaeridium complex</i> var. 1					3	2	
<i>Oligosphaeridium poculum</i>	5a	2	13	14	16	18	27
<i>Oligosphaeridium</i> aff. <i>pulcherrimum</i>				9			
<i>Oligosphaeridium</i> spp.		14	18	17	4	23	24
<i>Oligosphaeridium</i> with broken processes		7	19	19	13	7	20
Other dinocysts		15	20	15	21	20	5
<i>Palaecysta palmula</i>	5k		3				
<i>Palaeoperidinium cretaceum</i>						37	
Palynomorph A			57				8
Palynomorph B				11			
<i>Paragonyaulacysta capillosa</i>			4				
<i>Paragonyaulacysta</i> spp.			42	33	24	6	
<i>Pareodinia</i> spp.		23	14	25	34	21	38
<i>Phoberocysta neocomica</i>	5c	17	47		31		
<i>Prolixosphaeridiopsis spissa</i> (acritarch)			26				
<i>Pseudoceratium anaphrissum</i>	5m–o	46		16		31	
<i>Pseudoceratium pelfiferum</i>	5j	29	60	5	10	32	39
<i>Pseudoceratium</i> cf. <i>retusum</i> sensu Nøhr-Hansen, 1993						35	
<i>Pseudoceratium</i> spp.							51
<i>Rhynchodiniopsis aptiana</i>	5d, g	16	48		36		48
<i>Rhynchodiniopsis</i> spp.					25		
<i>Sepispinula?</i> <i>huguoniotii</i>			52				
<i>Scrinodinium campanula</i>				37		24	
<i>Sirmiodinium grossii</i>	6e, f	24	2	20	17	8	3
<i>Spiniferites</i> sp. 1	6d		54		29		30

(Continued)

Table 1. (Continued)

Palynomorph name in alphabetical order according to genus then species	Photo	Fig. S1	Fig. S2	Fig. S3	Fig. S4	Fig. S5	Fig. S6
<i>Spiniferites</i> spp.	6h		49	6			
<i>Stanfordella fastigiata</i>	6a	20	9	26	32	5	15
<i>Stanfordella ordocava</i>	6b, c		30		38	11	13
<i>Stiphrosphaeridium anthophorum</i>			63				
<i>Subtilisphaera perlucida</i>	6g			8		28	
<i>Tanyosphaeridium boletus</i>		34	45			29	53
<i>Tanyosphaeridium salpinx</i>		28	40		37	25	23
<i>Tanyosphaeridium</i> spp.					26		17
<i>Tubotuberella apatela</i>	6i–k	47	1,66	42	39	40	1
<i>Tubotuberella uncinata</i>		32					
<i>Tubotuberella</i> spp.	6l	38	11	43	11		2, 58
<i>Wallodinium luna</i>	6m						9
<i>Wrevittia helicoidea</i>		44	5				7
cf. <i>Wrevittia perforobtus</i>	6n–p	26	7			12	50
unidentifiable dinocysts		4	21	21		16	6

Rhynchodiniopsis aptiana (Fig. 5d, g), *Stanfordella fastigiata* (Fig. 6a), *Stanfordella ordocava* (Fig. 6b, c) and *Wrevittia perforobtus* (Fig. 6n–p). Notably, some of the well-known Lower Cretaceous markers, such as e.g. *Batioladinium longicornutum*, were not observed in the studied material.

The age-diagnostic taxa within the Helvetiafjellet Formation include *Odontochitina nuda* (Fig. 5e; Appendix 1f), *Pseudoceratium anaphrissum* (Fig. 5m–o; Appendix 1j), *Sirmiodinium grossii* (Fig. 6e, f; Appendix 1k) and *Subtilisphaera perlucida* (Fig. 6g; Appendix 1l). The Helvetiafjellet Formation is also characterized by low species richness, low relative abundance of dinocysts and a moderate reworking of Valanginian to Barremian dinocysts.

The age of the first (FOs) and last occurrences (LOs) as well as ranges of the key dinocysts in the context of existing literature are discussed in the Appendix.

7.a. Palynological framework for the Agardhfjellet Formation

The two lowermost samples from the DH5R core collected from the upper part of the Agardhfjellet Formation (at 458.0 and 440.0 m) are barren of dinocysts (online Supplementary Material Fig. S6). The sample at 410 m yields only a few, poorly preserved dinocysts (online Supplementary Material Fig. S6). In this sample, the co-occurrence of *Sirmiodinium grossii* and *Tubotuberella apatela* suggests a very broad Bathonian – early Valanginian age (e.g. Costa & Davey, 1992). Our dinocyst-derived age constraint is therefore not as good as the age based, for example, on macrofossils, which dates this part of the Agardhfjellet Formation as Ryazanian (Wierzbowski et al. 2011).

7.b. Palynological framework for the Rurikfjellet Formation

The distribution of dinocysts in the Rurikfjellet Formation (except the Myklegardfjellet Bed; Fig. 1) from the studied sites suggests that this formation is of early Valanginian to possibly earliest Barremian age (Fig. 8).

The dinocyst assemblages in the DH1 and DH2 cores are characterized by poor preservation, low diversity and low dinocyst abundance. Both cores penetrate the c.150 m thick gravity flow deposits of the Adventpynten member (Grundvåg et al. 2017) that yield a number of reworked taxa. In the DH2 core, the lowermost samples from the Rurikfjellet Formation yield only a single highly corroded *Oligosphaeridium* specimen (possibly *O. complex* or *O. asterigerum*). Thus, this interval is tentatively dated as Valanginian or younger (online Supplementary Material Fig. S5). The two lowermost samples from the DH1 well (corresponding to the base of the Rurikfjellet Formation according to Grundvåg et al. 2017) also yield *O. complex* (online Supplementary Material Fig. S4). Furthermore, the sample at 414.0 m yields *Gochteodinia villosa* subsp. *multifurcata* while the sample at 410.2 m yields *Muderongia tetracantha* (online Supplementary Material Fig. S4). Thus, this interval is of Valanginian–Hauterivian age. The presence of *Endoscrinium hauterivianum* between 270.0 and 221.0 m implies that this interval is of early Hauterivian to earliest late Hauterivian age (see below). In summary, in the DH1 core (i.e. 414.0 to 221.0 m depth) the Rurikfjellet Formation is dated as Valanginian – earliest late Hauterivian (online Supplementary Material Fig. S4).

We find the best-constrained age for the basal part of the Rurikfjellet Formation (early Valanginian) to be represented by the Myklegardfjellet outcrop section (the interval from the base of the section up to level 60.0 m; online Supplementary Material Fig. S2). This notion is based on the co-occurrence of *Palaecysta palmula* and *O. complex* in the lowermost sample at 0.05 m. The early Valanginian age for the base of the Rurikfjellet Formation confirms previous observations (Bjærke, 1978; Århus, 1992).

The LO of the stratigraphically persistent *T. apatela* at 60.0 m in the Myklegardfjellet outcrop section is used here as a marker for the top of the early Valanginian, since most records agree that this bio-event is close to the early–late Valanginian boundary (see below; Fig. 7). This age assignment is in agreement with the

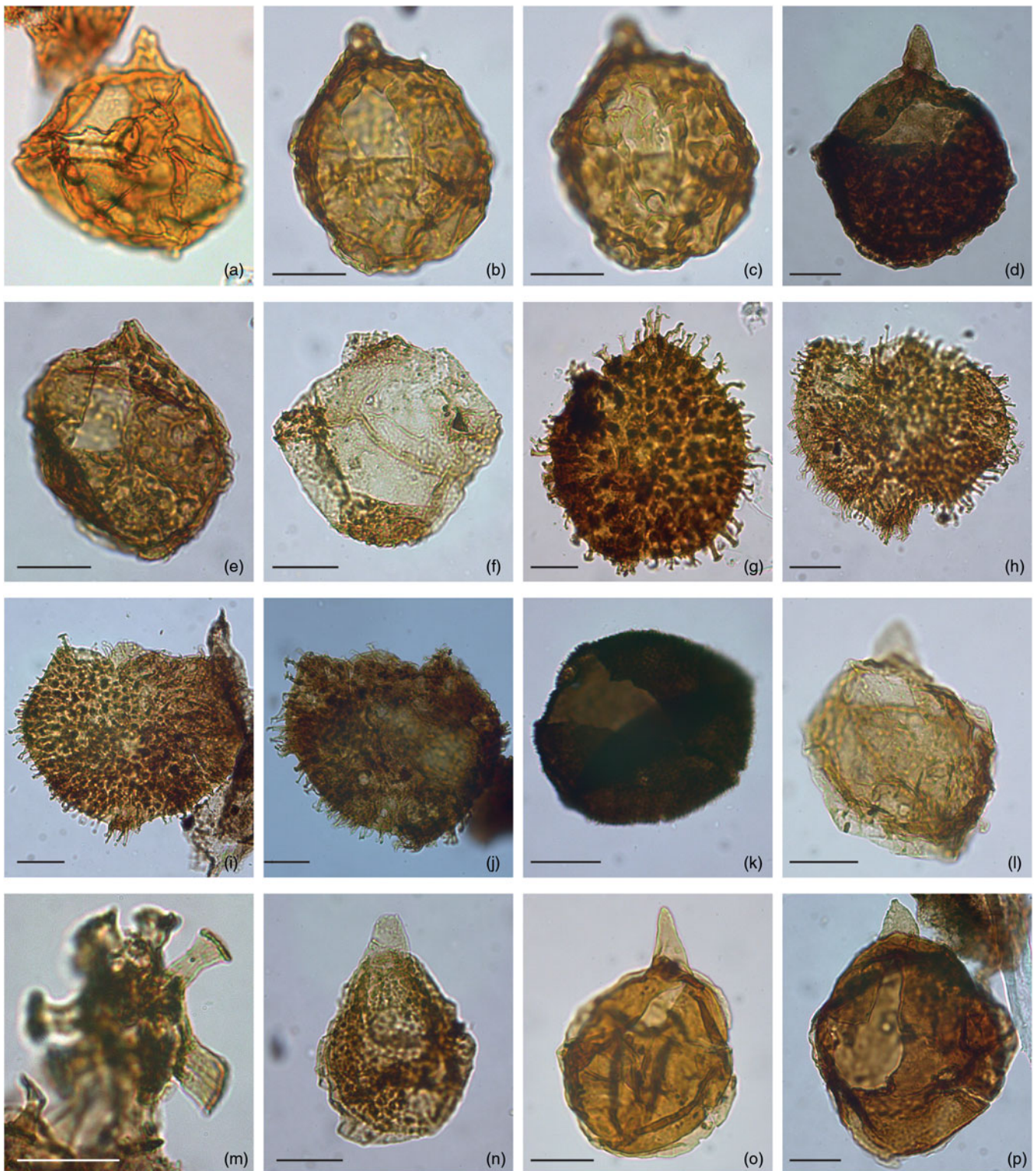


Fig. 3. Photographs of the most characteristic dinoflagellate cysts observed in the Rurikfjellet and Helvetiafjellet formations in the present study. Scale bars on all photographs represent 20 μm . MC – microscope coordinates with the A-point of 0.4×90.3 (XM1 \times YM1). For details, see Śliwińska (2019). (a) A dinocyst, Bohemanflya outcrop section, level 99.29 m, sample 26291-7; MC 102×42.2 . (b) *Apteodinium spongiosum*, high focus and (c) low focus, Bohemanflya outcrop section, level 25.00 m, sample 28450-9; MC 25×108.7 . (d) *Apteodinium spongiosum*, very dark, Myklegardfjellet outcrop section, level 30.00 m, sample 27007-6; MC 32×109.1 . (e) *Apteodinium spongiosum*, Myklegardfjellet outcrop section, level 120.00 m, sample 27013-9; MC 51.4×105.5 . (f) *Atopodinium haromense*; Myklegardfjellet outcrop section, level 120.00 m, sample 27013-9; MC 42.7×102.3 . (g) *Circulodinium distinctum*, Myklegardfjellet outcrop section, level 105.00 m, sample 27012-6; MC 29.3×91.6 . (h) *Circulodinium distinctum*, Myklegardfjellet outcrop section, level 120.00 m, sample 27013-9; MC 17.5×105.5 . (i) *Circulodinium distinctum*, Bohemanflya outcrop section, level 28.00 m, sample 28449-8; MC 44.7×96.7 . (j) *Circulodinium distinctum*, Bohemanflya outcrop section, level 7.00 m, sample 27005-4; MC 37.2×99.4 . (k) *Dissiliodinium acmeum*, Myklegardfjellet outcrop section, level 120.00 m, sample 27013-9; MC 25.5×110 . (l) *Endoscrinium* sp. 1 Bohemanflya outcrop section, level 25.00 m, sample 28450-9; MC 25.5×110 . (m) *Discorsia nannus*, Myklegardfjellet outcrop section, level 120.00 m, sample 27013-9; MC 49×103.3 . (n) *Dingodinium cerviculum*, Myklegardfjellet outcrop section, level 75.00 m, sample 27010-4; MC 47×108.5 . (o) *Endoscrinium hauterivianum*, Bohemanflya outcrop section, level 36.00 m, sample 28448-7; MC 33.8×102.2 . (p) *Endoscrinium hauterivianum*, Myklegardfjellet outcrop section, level 120.00 m, sample 27013-9; MC 42×102.4 .

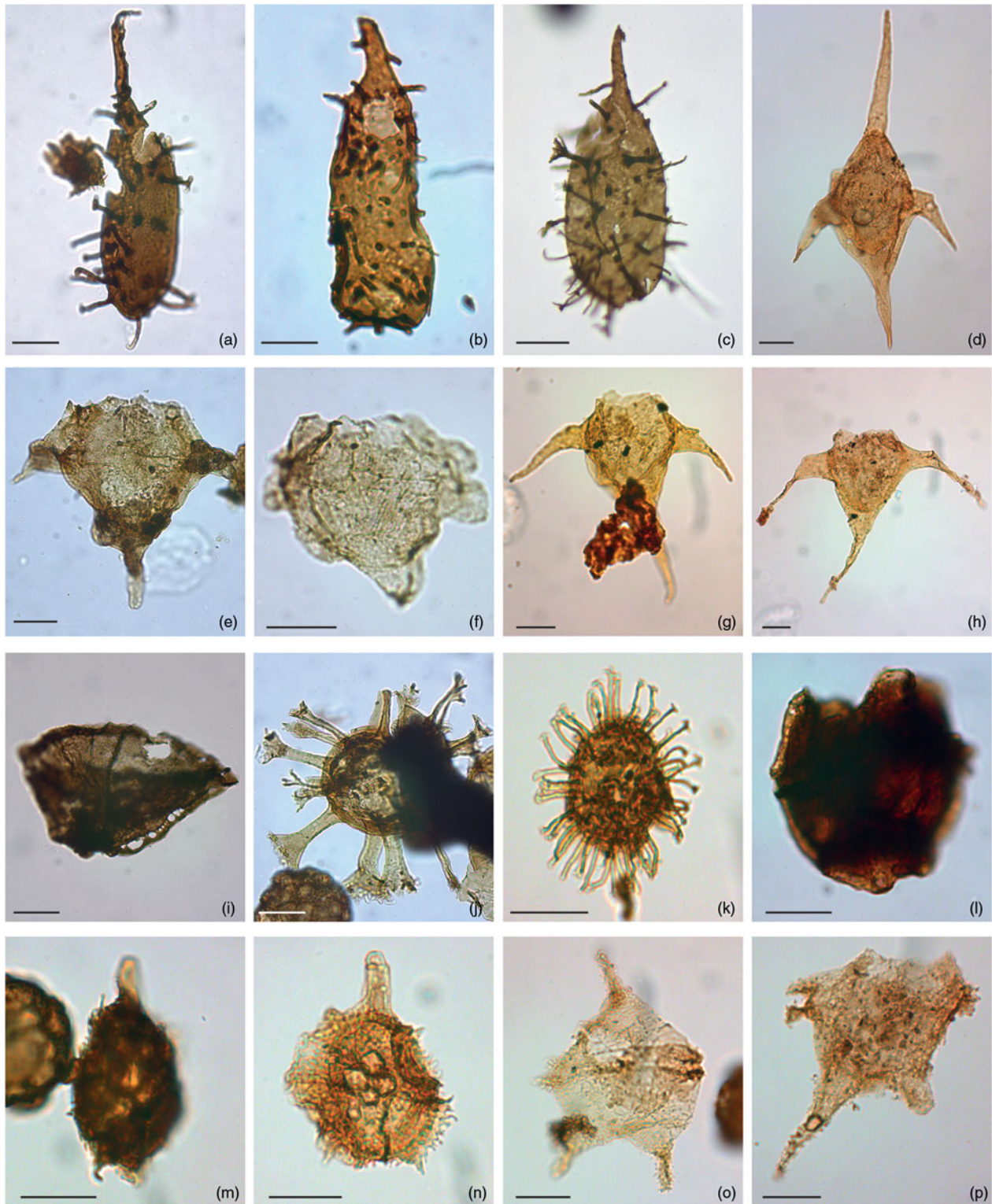


Fig. 4. Photographs of the most characteristic dinoflagellate cysts observed in the Rurikfjellet and Helvetiafjellet formations in the present study. Scale bars on all photographs represent 20 μm . MC – microscope coordinates with the A-point of 0.4×90.3 (XM1 \times YM1). For details, see Śliwińska (2019). (a) *Gochteodinia villosa* subsp. *multifurcata*, Myklegardfjellet outcrop section, level 15.00 m, sample 27006-5; MC 36.3 \times 114. (b) *Gochteodinia villosa*, DH5R core, depth 350.00 m, sample 26197-6; MC 22.5 \times 96.2. (c) *Gochteodinia villosa* subsp. *multifurcata*, Myklegardfjellet outcrop section, level 15.00 m, sample 27006-5; MC 36 \times 107. (d) *Muderongia tetracantha*, Bohemanflya outcrop section, level 127.50 m, sample 26290-8; MC 44 \times 110.6. (e) *Muderongia australis*, Myklegardfjellet outcrop section, level 120.00 m, sample 27013-9; MC 31.4 \times 108.5. (f) *Muderongia simplex*, Myklegardfjellet outcrop section, level 105.00 m, sample 27012-6; MC 33 \times 105.8. (g) A transitional form between *Muderongia tetracantha* and *Muderongia extensiva*, Bohemanflya outcrop section, level 46.00 m, sample 26293-5, MC 24.5 \times 111. (h) *Muderongia extensiva*, Bohemanflya outcrop section, level 46.00 m, sample 26293-7; MC 18.5 \times 108.4. (i) *Isthmocystis distincta*, Myklegardfjellet outcrop section, level 7.00 m, sample 27005-4; MC 28 \times 102.3. (j) *Kleithrisphaeridium eoinodes*, Myklegardfjellet outcrop section, level 90.00 m, sample 27011-8; MC 25.2 \times 103. (k) *Kiokansium unituberculatum*, Bohemanflya outcrop section, level 127.50, sample 26290-6; MC 31 \times 107.3. (l) *Meiourugonyaulax stoveri*, DH5R core, depth 258.00 m, sample 26194-5; MC 24 \times 107.8. (m) Poorly preserved *Nelchinopsis kostromiensis*, Bohemanflya outcrop section, level 99.29 m, sample 26291-7; MC 52.4 \times 109. (n) *Nelchinopsis kostromiensis*, Bohemanflya outcrop section, level 55.25 m, sample 26292-7; MC 51.5 \times 95.5. (o) *Nyctericysta? pannosa*, Bohemanflya outcrop section, level 99.29 m, sample 26291-7; MC 43 \times 102.7. (p) *Nyctericysta? pannosa*, Bohemanflya outcrop section, level 127.50 m, sample 26290-8; MC 50.2 \times 100.

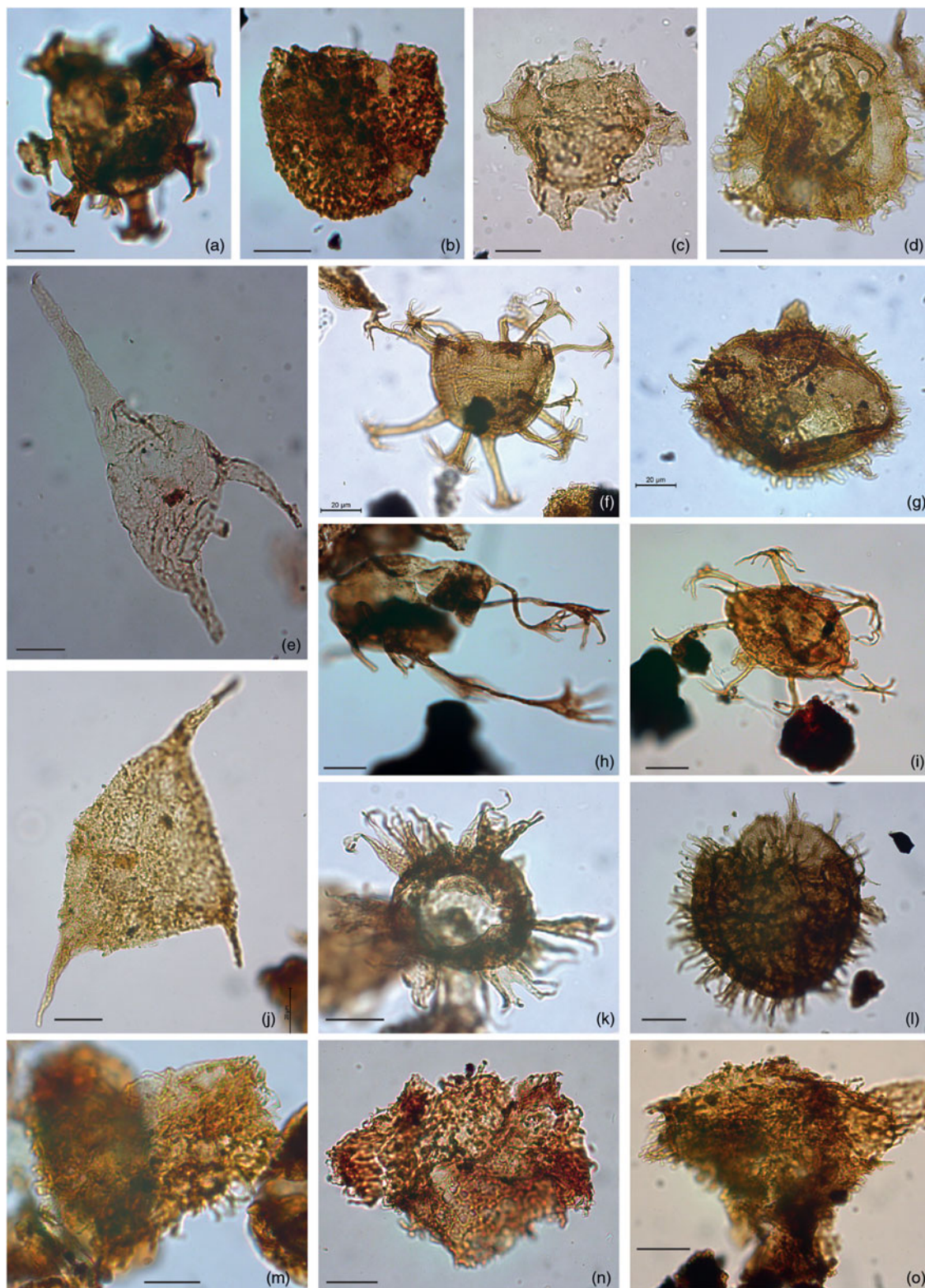


Fig. 5. Photographs of the most characteristic dinoflagellate cysts observed in the Rurikfjellet and Helvetiafjellet formations in the present study. Scale bars on all photographs represent 20 μm . MC – microscope coordinates with the A-point of 0.4×90.3 (XM1 \times YM1). For details, see Śliwińska (2019). (a) *Oligosphaeridium poculum*, DH5R core, depth 320.00 m, sample 26196-7; MC 58.2 \times 97.1. (b) Questionable *Escharisphaeridia rudis*, DH5R core, depth 288.00 m, sample 26195-7; MC 36.7 \times 112.5. (c) *Phoberocysta neocomica*, Myklegardfjellet outcrop section, level 90.00 m, sample 27009-6; MC 24.3 \times 113.8. (d) *Rhynchodiniopsis aptiana*, Bohemanflya outcrop section, level 5.00 m, sample 28453-7; MC 31.7 \times 101. (e) *Odontochitina nuda*, DH2 core, depth 141.80 m, sample 26510-9; MC 42 \times 105.2. (f) *Oligosphaeridium abaculum*, Myklegardfjellet outcrop section, level 75.00 m, sample 27010-5; MC 48.5 \times 105.5. (g) *Rhynchodiniopsis aptiana*, Myklegardfjellet outcrop section, level 105.00 m, sample 27012-6; MC 20.3 \times 107.5. (h) *Oligosphaeridium complex* with ‘palm-like’ terminations of processes, DH1, depth 258.90 m, sample 26285-7; MC 32.8 \times 97.1. (i) *Oligosphaeridium asterigerum*, Bohemanflya outcrop section, level 99.29 m, sample 26291-7; MC 44.7 \times 94.3. (j) *Pseudoceratium pelliferum*, Bohemanflya outcrop section, level 36.00 m, sample 28448-7; MC 37 \times 106.5. (k) *Palaeocysta palmula*, Myklegardfjellet outcrop section, level 0.05 m, sample 27004-8; MC 53 \times 107.5. (l) *Cyclonephelium cuculliforme sensu* Århus, 1990, Myklegardfjellet outcrop section, level 15.00, sample 27006-3; MC 30.2 \times 101. (m) Questionable *Pseudoceratium anaphrissum* Bohemanflya outcrop section, level 132.63 m, sample 26289-8; MC 37.8 \times 95.5. Also shown in figure 15.P in Grundvåg et al. (2019). (n) *Pseudoceratium anaphrissum*, Ullaberget outcrop section, level 104.00 m, sample 28482-7; MC 40.6 \times 111.8. (o) Questionable, poorly preserved *Pseudoceratium anaphrissum*, DH2 core, depth 149.50 m, sample 26511-11; MC 34.5 \times 110.5. Also shown in figure 15.H in Grundvåg et al. (2019).

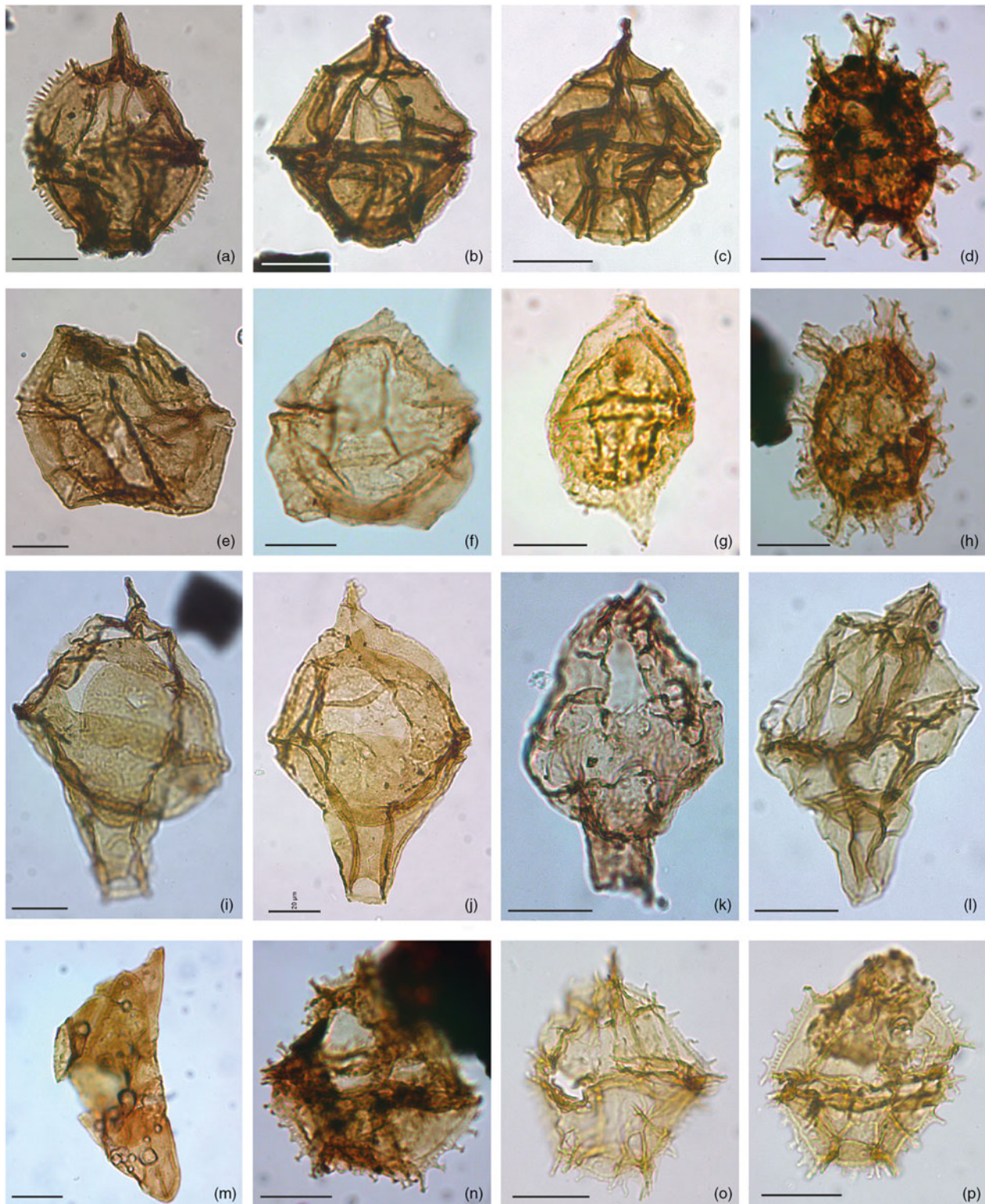


Fig. 6. Photographs of the most characteristic dinoflagellate cysts observed in the Rurikfjellet and Helvetiafjellet formations in the present study. Scale bars on all photographs represent 20 μm . MC – microscope coordinates with the A-point of 0.4×90.3 (XM1 \times YM1). For details, see Śliwińska (2019). (a) *Stanfordella fastigiata*, Myklegardfjellet outcrop section, level 30.00 m, sample 27007-6; MC 50.4 \times 103.5. (b) *Stanfordella ordocava*, Myklegardfjellet outcrop section, level 15.00 m, sample 27006-5; MC 31.6 \times 111. (c) *Stanfordella ordocava*, DH5R core, depth 380.00 m, sample 26198-6; MC 55.5 \times 102.4. (d) *Spiniferites* sp. 1, DH5R core, depth 194.00 m, sample 26192-7; MC 36.9 \times 102. (e) *Sirmiodinium grossii*, Myklegardfjellet outcrop section, level 30.00 m, sample 27007-6; MC 30.3 \times 104.2. (f) *Sirmiodinium grossii*, DH1, depth 258.90 m, sample 26285-7; MC 29.4 \times 109. (g) *Subtilisphaera perlucida*, DH2 core, depth 186.55 m, sample 26513-9; MC 36.7 \times 92.6. Also shown in figure 15.G in Grundvåg et al. (2019). (h) *Spiniferites?* DH5R core, depth 194.00 m, sample 26192-7; MC 50.8 \times 101.2. (i) *Tubotuberella apatela*, Myklegardfjellet outcrop section, level 30.00 m, sample 27007-6; MC 30.6 \times 105. (j) *Tubotuberella apatela*, Myklegardfjellet outcrop section, level 0.05 m, sample 27004-8; MC 34.5 \times 109.4. (k) *Tubotuberella apatela*, DH2 core, depth 232.00 m, sample 26516-9; MC 19.4 \times 93.3. (l) *Tubotuberella* sp. DH5R core, depth 380.0 m, sample 26198-6; MC 48 \times 98.7. (m) *Wallodinium luna*, DH5R core, depth 350.0 m, sample 26197-6; MC 36.5 \times 102.4. (n) *Wrevittia perforobtusata*, DH5R core, depth 194.00 m, sample 26192-7; MC 29.9 \times 102.6. (o) *Wrevittia perforobtusata*, Bohemanflya outcrop section, level 55.25 m, sample 26292-8; MC 50.3 \times 101.7. (p) *Wrevittia perforobtusata*, Bohemanflya outcrop section, level 36 m, sample 28448-7; MC 40.5 \times 98.6.

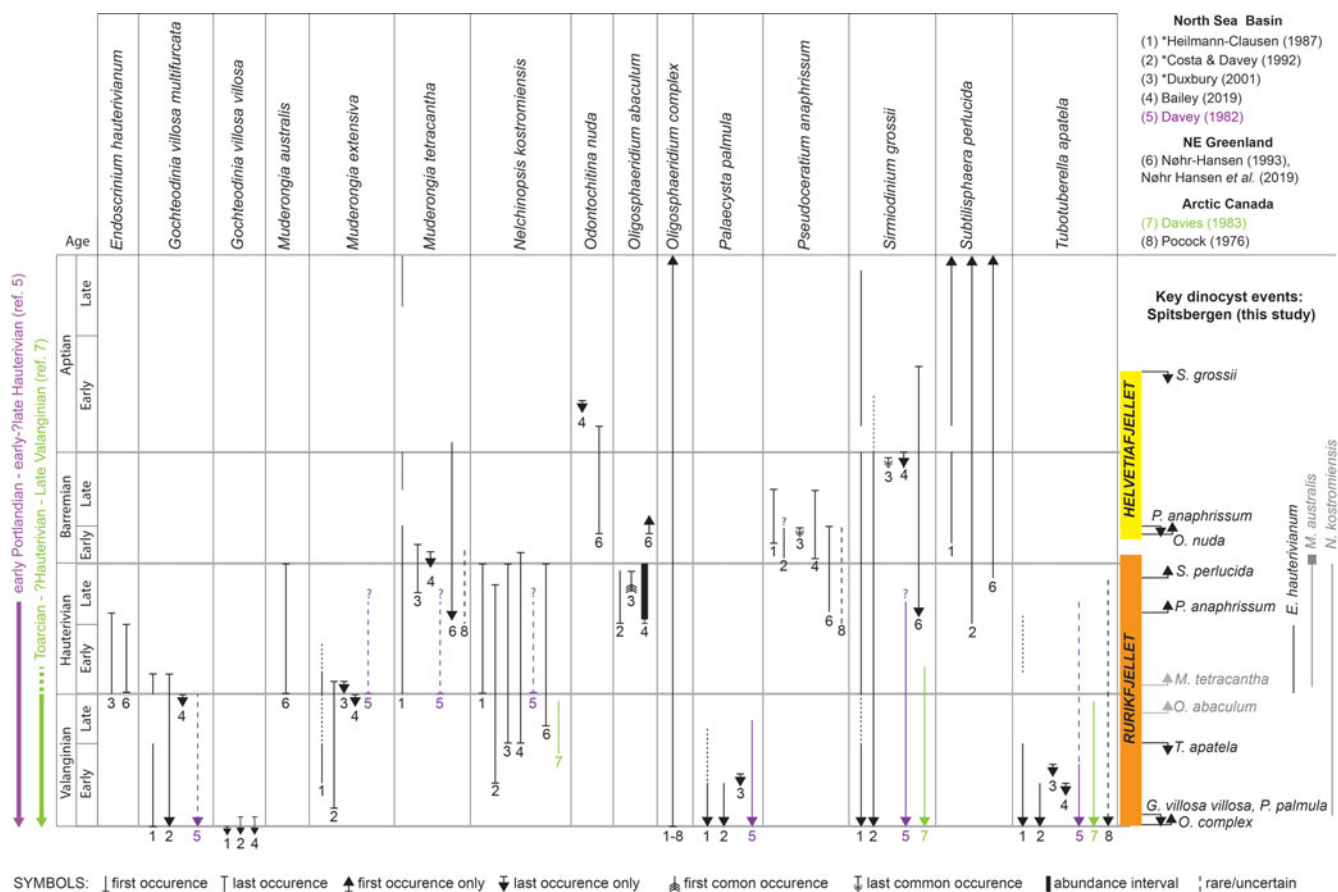


Fig. 7. The stratigraphic ranges and/or first and last occurrences of the age-diagnostic dinoflagellate cysts (dinocysts) from the Boreal and European Boreal Realm, and the key events recognized in this study (to the right). Key dinocyst events in Spitsbergen: primary markers (black), secondary markers (grey). The figure shows a compilation of the most characteristic dinocysts from the Rurikfjellet and Helvetiafjellet formations discussed in the present study. Heilmann-Clausen (1987), Costa & Davey (1992) and Duxbury (2001) plotted the dinocyst ranges against the ammonite zonation (marked with asterisk). All these authors considered the *Simbirskites variabilis* ammonite zone as earliest Barremian, whilst today it is considered to be Hauterivian (Ogg *et al.* 2016). Nøhr-Hansen *et al.* (2019) updated the zonation proposed previously by Nøhr-Hansen (1993), and provided ages in GTS2016. Note that the study by Davey (1982) does not cover sediments younger than lower–upper Hauterivian, while the study by Davies (1983) does not cover sediments younger than upper Valanginian.

presence of a *Tollia* (*Neocraspedites*) aff. *subtilis* ammonite of middle early Valanginian age found at 47.30 m (P. Alsen & M. E. Jelby, unpub. data).

In the DH5R core, the top of the stratigraphically persistent *Gochteodinia villosa* subsp. *villosa* is at 320.0 m, and it co-occurs with *O. complex* in the interval from 380.0 to 320.0 m. Based on these occurrences, we date this interval as earliest Valanginian. Placing the early–late Valanginian boundary close to the top of the persistent occurrence of these two taxa is in agreement with the observations by Århus (cf. fig. 2 in Århus, 1992, and enclosure 2 in Århus, 1988).

We place the base of the Hauterivian at the FO of *E. hauterivianum* (Fig. 8). The FO of *E. hauterivianum* is followed by the FO of *Muderongia tetracantha*, another important marker for the Hauterivian (e.g. Costa & Davey, 1992) (Fig. 7). The stratigraphic range of *E. hauterivianum* observed in five sites (DH1, DH2, DH5R, Bohemanflya and Myklegardfjellet) in the middle to upper part of the Rurikfjellet Formation dates this part of the unit to the early Hauterivian – earliest late Hauterivian (online Supplementary Material Figs S4, S5; Fig. 4). Grøsfjeld (1991) noted that *E. hauterivianum* (as *Apteodinium* sp. A of Bjørke, 1978; Appendix 1a) is also present in several other outcrop sections of the Rurikfjellet Formation including Janusfjellet, Forkastningsfjellet and Helvetiafjellet.

Many samples from the uppermost part of the Rurikfjellet Formation in the DH1, DH2 and DH5R cores are characterized by low dinocyst abundance and relatively low species richness. The best age constraint for the top of the formation is therefore based on outcrop sections. The upper part of the Rurikfjellet Formation is dated to the late Hauterivian – earliest Barremian. The youngest part of the formation dated to the early Barremian is observed at Ullaberget and Bohemanflya.

In the Ullaberget outcrop section, two samples at 0.0 and 2.0 m, collected from the top of the Rurikfjellet Formation, yield *Pseudoceratium anaphrissum* and *Subtilisphaera perlucida*. The sample at 0.0 m additionally yields *Nelchinopsis kostromiensis*, *P. anaphrissum* and *S. perlucida*, which have their FOs close to the Hauterivian – Barremian boundary (online Supplementary Material Fig. S3). In the North Sea Basin, the LO of *N. kostromiensis* and the FO of *P. anaphrissum* are two important bio-events for recognition of the Hauterivian–Barremian boundary. Typically, the LO of *N. kostromiensis* marks the top of the Hauterivian, while the FO of *P. anaphrissum* marks the base of the Barremian (e.g. Costa & Davey, 1992). However, in some studies both bio-events are reported from the lowermost Barremian (Heilmann-Clausen, 1987; Århus *et al.* 1990; Smelror *et al.* 1998; Bailey, 2019) or the upper Hauterivian (Nøhr-Hansen, 1993; Nøhr-Hansen *et al.* 2019). In the North Sea, the ranges of these two species either

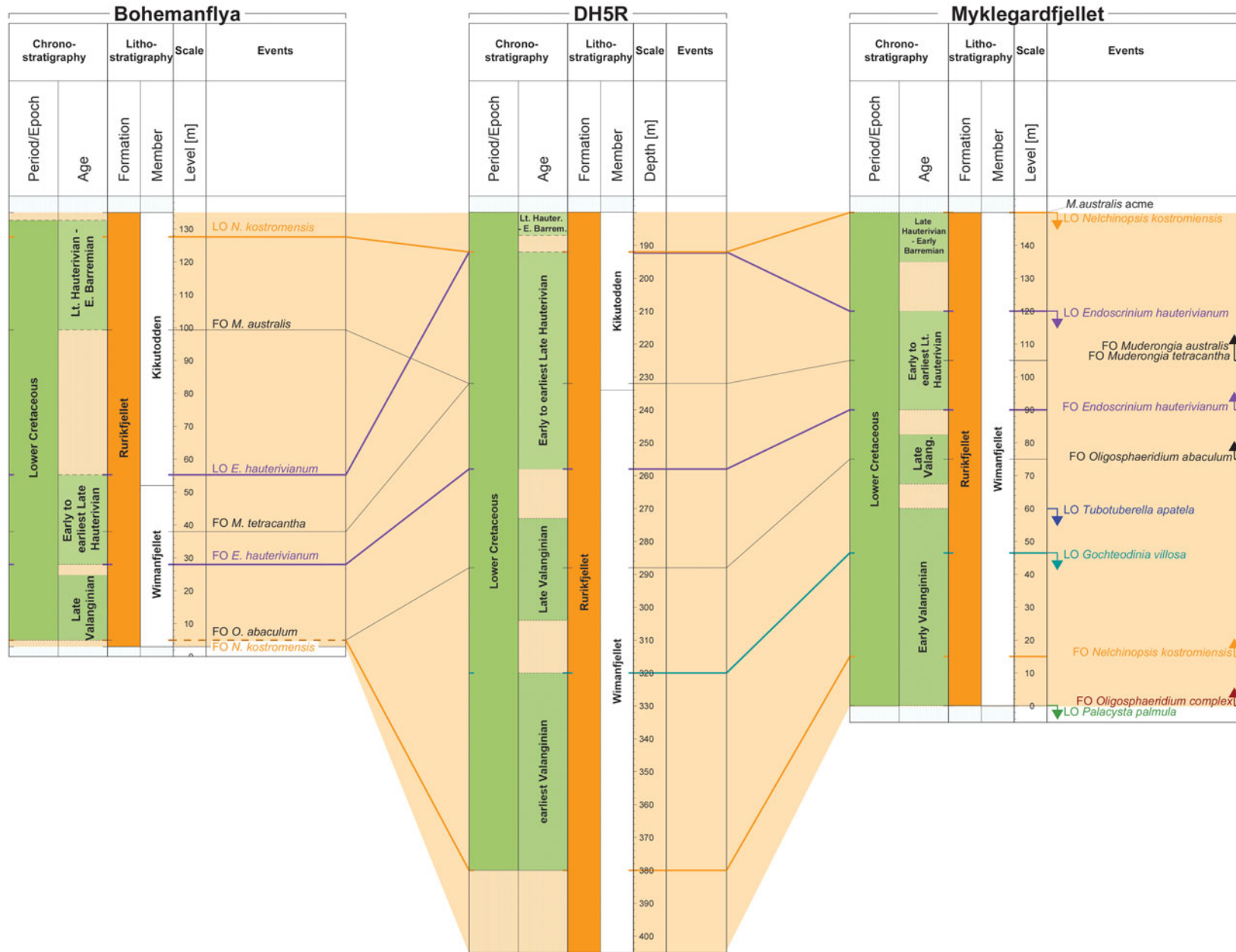


Fig. 8. The spatial distribution of the age-diagnostic (colour coded) and secondary dinocyst events (black) within the Rurikfjellet Formation. The correlation between the Bohemanflya, DH5R core and Myklegardfjellet outcrop section, i.e. from NW to SE.

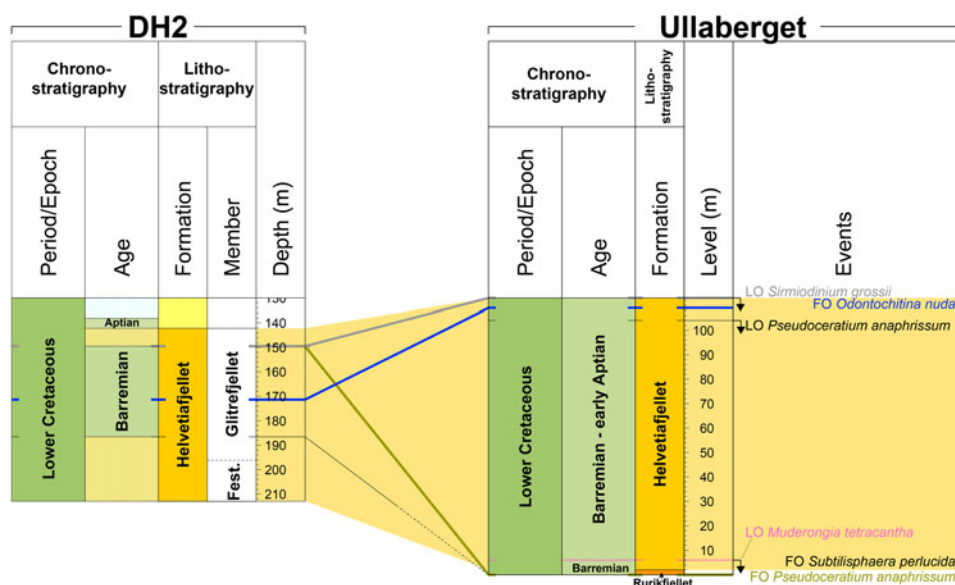


Fig. 9. The spatial distribution of the age-dagnostic dinocyst events within the Helvetiafjellet Formation. The correlation between the Ullaberget outcrop section and DH2 core.

overlap (Costa & Davey, 1992) or do not (Bailey, 2019). Overlapping ranges of the two taxa have been observed in NE Greenland (Nøhr-Hansen, 1993; Nøhr-Hansen *et al.* 2019). An overlap of the stratigraphic ranges of the two species was previously reported from the Barents Sea (well 7245/9-U-1) (fig. 5 in Århus *et al.* 1990). Based primarily on the foraminifera assemblage, the overlap interval was dated as early Barremian (Århus *et al.* 1990). However, these authors recognized that the presence of *Buchia sublaevis* bivalves within the same interval was problematic (p. 173 in Århus *et al.* 1990), because *Buchia* extends only into the Hauterivian (Zakharov, 1987). In summary, these observations give three possibilities for assigning an age to the LO of *N. kostromiensis* and the FO of *P. anaphrissum*: (i) In Spitsbergen, the Barents Sea and NE Greenland, *P. anaphrissum* appears in the upper Hauterivian; (ii) in Spitsbergen and the Barents Sea region, *N. kostromiensis* has a longer range reaching the lowermost Barremian; or (iii) *N. kostromiensis* occurring in the lower Barremian strata is reworked. We consider the first possibility to be the most plausible, since this is in agreement with other studies from the Arctic region (NE Greenland, Barents Sea and Arctic Canada; cf. Fig. 7).

In the three uppermost samples from the Bohemanflya outcrop section (99.29 m to 132.63 m), we found a common to abundant dinocyst taxon previously recorded as *Nyctericysta? pannosa* by Grøsfjeld (1991). However, we observe that *N.? pannosa* from Bohemanflya (Fig. 4o, p) with its generally less pronounced lateral horns differs from the holotype, which was described from 'middle Barremian' strata from the Speeton Clay in England (Duxbury, 1980). Nevertheless, Grøsfjeld (1991) and this study show the only records of this taxon outside the type area. The restricted occurrence of *N.? pannosa*, limited to the Bohemanflya section on Spitsbergen (Grøsfjeld, 1991; this study) and to the Speeton Clay in England (Duxbury, 1980), could suggest that the distribution of the taxon is controlled by some environmental factors. *Oligosphaeridium abaculum* is another taxon which has a significantly different range in Spitsbergen than in surrounding basins (Appendix 1g). In Spitsbergen the taxon appears in the Valanginian, i.e. much earlier than in the North Sea and North-East Greenland (Fig. 7). The diachroneity of the event may also be caused by the local environmental changes.

Based on the LO of *N. kostromiensis* at 127.58 m and the presence of *N.? pannosa* between 99.29 m and 132.63 m, the interval is dated as latest Hauterivian – early Barremian.

In the topmost sample of the Myklegardfjellet outcrop section at 150.0 m, we observed an acme of *M. australis*. We consider this acme to be time-equivalent to the *M. australis* acme observed in the Barents Sea by Århus *et al.* (1990). Thus, we date this level as late Hauterivian – early Barremian.

Our new age framework for the Rurikfjellet Formation based on the dinocyst stratigraphy is in agreement with previous studies from the study area (e.g. Bjærke, 1978; Thusu, 1978; Århus, 1992; Midtkandal *et al.* 2016), which dated the majority of the Rurikfjellet Formation as Valanginian–Hauterivian. Specifically, the Rurikfjellet Formation at the Janusfjellet outcrop section was previously dated as early Valanginian – late Hauterivian (Århus, 1992). We observe that our dinocyst distribution of the Myklegardfjellet outcrop section (online Supplementary Material Fig. S2) resembles the distribution of dinocysts from Janusfjellet (enclosure 2 in Århus, 1988). Furthermore, our results confirm the observation by Grøsfjeld (1991) that the topmost part of the Rurikfjellet Formation is most likely of early Barremian age. Some reworking is present, which is minor compared to the reworking in the Helvetiafjellet Formation (online Supplementary Material Figs S1–S6).

7.c. Palynological framework for the Helvetiafjellet Formation

We observe that the dinocyst assemblages of the Helvetiafjellet Formation are highly impoverished and yield a number of taxa reworked from the Rurikfjellet Formation. The reworking of Pliensbachian to early Oxfordian dinocysts within the Helvetiafjellet Formation was observed previously on Kong Karls Land (Smelror *et al.* 2018). Redeposition is, however, not surprising, considering that the study area was uplifted and subaerially exposed in the Barremian with large parts of the Svalbard platform being subjected to erosion (Fig. 2).

Based on the presence of *Odontochitina nuda*, *Pseudoceratium anaphrissum*, *Sirmiodinium grossii* and *Subtilisphaera perlucida*, the Helvetiafjellet Formation is dated here as Barremian to possibly

early Aptian (online Supplementary Material Figs S3, S5; Fig. 9). The boundary between the Rurikfjellet and Helvetiafjellet formations is dated as early Barremian. Owing to the low diversity of the assemblages and rarity of dinocysts, it is not possible to precisely place the Barremian–Aptian boundary.

Our age assignment of the Helvetiafjellet Formation is in agreement with a recent stable carbon isotope ($\delta^{13}\text{C}$) stratigraphic study of the Festningen outcrop section (Vickers et al. 2016). These authors interpreted that the Helvetiafjellet Formation is of Barremian to earliest Aptian age. Another study, based on the U–Pb dating of a bentonite in the DH3 core (at 156.89 m in the middle part of the Helvetiafjellet Formation) suggested an age of 123.3 ± 0.2 Ma for this particular bed (Corfu et al. 2013), corresponding to the late early Aptian (Ogg et al. 2016). However, the biostratigraphic framework of this study and Midtkandal et al. (2016) suggest that this part of the succession is rather of Barremian age. Nevertheless, the existing studies (e.g. Corfu et al. 2013; Midtkandal et al. 2016; Vickers et al. 2016) collectively agree that the Helvetiafjellet Formation is of Barremian – early Aptian age.

8. Conclusions

The Rurikfjellet and Helvetiafjellet formations on Spitsbergen, Svalbard, have been studied in the DH1, DH2 and DH5R onshore cores as well as in the Bohemanflya, Myklegardfjellet and Ullaberget outcrop sections. Our study suggests an early Valanginian – early Barremian age for the Rurikfjellet Formation and a Barremian–Aptian age for the overlying Helvetiafjellet Formation. We provide a number of age-diagnostic dinocyst bio-events for age determination of the Rurikfjellet and Helvetiafjellet formations. The preservation of dinocysts is better and the diversity of assemblages is significantly higher in the offshore to shallow-marine Rurikfjellet Formation than in the fluvio-deltaic to paralic Helvetiafjellet Formation.

We observe some reworked dinocysts within the Helvetiafjellet Formation, possibly from the Rurikfjellet Formation. The presence of reworked dinocysts implies that any proxy records performed on bulk sediments (e.g. $\delta^{13}\text{C}$, biomarkers) across the Barremian–Aptian transition on Spitsbergen should be interpreted with care, since the signal may be biased.

We further observe that the distribution of *N.?* *pannosa* and *O. abaculum* (Appendix 1g) is most likely controlled by local palaeoenvironmental variations. For a better understanding of these records, further palaeoenvironmental proxy data from the area are required.

The dinocyst assemblages in the three samples collected from the Agardhfjellet Formation are too impoverished to provide a reliable age constraint on the boundary between the Rurikfjellet and Agardhfjellet formations.

Our age model is in agreement with the existing stratigraphic studies carried out in the study area. Notably, our study provides the first comprehensive, semi-quantitative dataset of the distribution of dinocysts within the Lower Cretaceous (Valanginian–Aptian) succession on Spitsbergen.

Acknowledgements. This research was carried out within the LoCrA consortium (<https://wp.ux.uis.no/locra>), generously sponsored by 22 industry partners. Thanks are extended to Annette Ryge, Charlotte Olsen and Dorthe Samuelsen (GEUS) for preparation of palynological slides. S.-A. Grundvåg acknowledges funding from the ARCEX project (Research Centre for Arctic Petroleum Exploration), which is funded by the Research Council of

Norway (grant number 228107). Figures 8 and 9, and S1–S6 were prepared using the StrataBugs v2.0 charts. We thank reviewers Wiesława Viola Radmacher and Kari Grøsfeld as well as editor Jennifer Galloway for valuable comments and suggestions, which improved this manuscript.

Supplementary material. To view supplementary material for this article, please visit <https://doi.org/10.1017/S0016756819001249>

References

- Alberti G (1959) Zur Kenntnis der Gattung Deflandrea Eisenack (Dinoflag.) in der Kreide und im Alttertiär Nord- und Mitteleuropas. *Mitteilungen aus dem Geologischen Staatsinstitut in Hamburg* **28**, 93–105.
- Alberti G (1961) Zur Kenntnis mesozoischer und alttertiärer Dinoflagellaten und Hystrichosphaerideen von Nord- und Mitteleuropa sowie einigen anderen europäischen Gebieten. *Palaeontographica, Abteilung A* **116**, 1–58.
- Alsen P, Jelby ME, Śliwińska KK and Mutterlose J (2019) An Early Cretaceous stratigraphic marker fossil in the High Arctic: the belemnite *Arctoteuthis bluetgeni*. *Geological Magazine*, published online 8 October 2019. doi: [10.1017/S0016756819000803](https://doi.org/10.1017/S0016756819000803).
- Århus N (1988) Palynostratigraphy of some Bathonian–Hauterivian sections in the Arctic, with emphasis on the Janusfjellet Formation type section, Spitsbergen. *IKU-Report* 23.1252.11/01/88. Trondheim: Institutt for Kontinentalsokkelundersøkelser og Petroleumsteknologi, 139 pp.
- Århus N (1991) Dinoflagellate cyst stratigraphy of some Aptian and Albian sections from North Greenland, southeastern Spitsbergen and the Barents Sea. *Cretaceous Research* **12**, 209–25. doi: [10.1016/0195-6671\(91\)90035-B](https://doi.org/10.1016/0195-6671(91)90035-B).
- Århus N (1992) Some dinoflagellate cysts from the Lower Cretaceous of Spitsbergen. *Grana* **31**, 305–14. doi: [10.1080/00173139209429453](https://doi.org/10.1080/00173139209429453).
- Århus N, Kelly SRA, Collins JSH and Sandy MR (1990) Systematic palaeontology and biostratigraphy of two Early Cretaceous condensed sections from the Barents Sea. *Polar Research* **8**, 165–94.
- Århus N, Verdenius J and Birkelund T (1986) Biostratigraphy of a Lower Cretaceous section from Sklinnabanken, Norway, with some comments on the Andøya exposure. *Norsk Geologisk Tidsskrift* **66**, 17–43.
- Bailey D (2019) *Early Cretaceous Zonation*. Cumbria, UK: BioStrat Ltd. Available at: http://www.biostrat.org.uk/EK_Zones_2011postcon.pdf (Accessed: 15 May 2019).
- Bint AN (1986) Fossil Ceratiaceae: a restudy and new taxa from the mid-Cretaceous of the Western Interior, U.S.A. *Palynology* **10**, 135–80.
- Birkenmajer K, Pugaczewska H and Wierzbowski A (1979) The Janusfjellet Formation (Jurassic–Lower Cretaceous) at Myklegardfjellet, East Spitsbergen. *Palaeontologia Polonica* **43**, 107–40.
- Bjærke T (1978) Mesozoic palynology of Svalbard III. Dinoflagellates from the Rurikfjellet Member, Janusfjellet Formation (Lower Cretaceous) of Spitsbergen. *Palinologia, numero extraordinarium* **1**, 69–93.
- Bjærke T and Thusu B (1976) Cretaceous palynomorphs from Spitsbergenbanken NW Barents Shelf. *Norsk Polarinstitut Årbok* **1974**, 258–62.
- Bottini C and Erba E (2018) Mid-Cretaceous paleoenvironmental changes in the western Tethys. *Climate of the Past* **14**, 1147–63. doi: [10.5194/cp-14-1147-2018](https://doi.org/10.5194/cp-14-1147-2018).
- Bottini C, Erba E, Tiraboschi D, Jenkyns HC, Schouten S and Sinningh Damsté JS (2015) Climate variability and ocean fertility during the Aptian Stage. *Climate of the Past* **11**, 383–402. doi: [10.5194/cp-11-383-2015](https://doi.org/10.5194/cp-11-383-2015).
- Braathen A, Bælum K, Christiansen HH, Dahl T, Eiken O, Elvebakk H, Hansen F, Hanssen TH, Jochmann M, Johansen TA, Johnsen H, Larsen L, Lie T, Mertes J, Mørk A, Mørk MB, Nemeč W, Olausen S, Oye V, Rød K, Titlestad GO, Tveranger J and Vagle K (2012) The Longyearbyen CO₂ lab of Svalbard, Norway – initial assessment of the geological conditions for CO₂ sequestration. *Norsk Geologisk Tidsskrift* **92**, 353–76. doi: [10.1095/biolreprod.111.094433](https://doi.org/10.1095/biolreprod.111.094433).
- Brideaux WW (1977) Taxonomy of Upper Jurassic–Lower Cretaceous microplankton from the Richardson Mountains, District of Mackenzie, Canada. *Geological Survey of Canada Bulletin* **281**, 1–89. doi: [10.4095/102868](https://doi.org/10.4095/102868).

- Cookson IC and Eisenack A** (1960) Upper Mesozoic microplankton from Australia and New Guinea. *Palaeontology* **2**, 243–61.
- Corfu F, Polteau S, Planke S, Faleide JJ, Svensen H, Zayoncheck A and Stolbov N** (2013) U–Pb geochronology of Cretaceous magmatism on Svalbard and Franz Josef Land, Barents Sea large igneous province. *Geological Magazine* **150**, 1127–35. doi: [10.1017/S0016756813000162](https://doi.org/10.1017/S0016756813000162).
- Costa L** (1981) Palynostratigraphy, Upper Cretaceous to Lower Cretaceous in the wells 2/7-1 and 2/7-3. In *The Eldfisk Area* (ed. K Ofstad), pp. 1–34. Stavanger: Norwegian Petroleum Directorate Paper no. 30.
- Costa L and Davey RJ** (1992) Dinoflagellate cysts of the Cretaceous System. In *A Stratigraphic Index of Dinoflagellate Cysts* (ed. A Powell), pp. 99–153. British Micropalaeontological Society Publication Series. London: Chapman and Hall.
- Davey RJ** (1979a) The stratigraphic distribution of dinocysts in the Portlandian (latest Jurassic) to Barremian (early Cretaceous) of northwest Europe. *American Association of Stratigraphic Palynologists Contributions Series* **5B**, 49–81.
- Davey RJ** (1979b) Two new Early Cretaceous dinocyst species from the northern North Sea. *Palaeontology* **22**, 427–37.
- Davey RJ** (1982) Dinocyst stratigraphy of the latest Jurassic to Early Cretaceous of the Haldage No. 1 borehole, Denmark. *Danmarks Geologiske Undersøgelse, Series B*, **6**, 1–57.
- Davey RJ** (1988) Palynological zonation of the Lower Cretaceous, Upper and uppermost Middle Jurassic in the northwestern Papuan Basin of Papua New Guinea. *Geological Survey of Papua New Guinea, Memoir* **13**, 1–77.
- Davey RJ and Williams GL** (1966) V. The genus *Hystrichosphaeridium* and its allies. In *Studies on Mesozoic and Cainozoic Dinoflagellate Cysts* (eds RJ Davey, C Downie, WAS Sarjeant and GL Williams), pp. 53–106. London: British Museum (Natural History) Geology, Bulletin, Supplement 3.
- Davies EH** (1983) The dinoflagellate Opelet-zonation of the Jurassic–Lower Cretaceous Sequence in the Sverdrup Basin, Arctic Canada. *Geological Survey of Canada Bulletin* **359**, 1–59.
- De Lurio JL and Frakes LA** (1999) Glendonites as a paleoenvironmental tool: implications for early Cretaceous high latitude climates in Australia. *Geochimica et Cosmochimica Acta* **63**, 1039–48. doi: [10.1016/S0016-7037\(99\)00019-8](https://doi.org/10.1016/S0016-7037(99)00019-8).
- Dietmar Müller R and Spielhagen RF** (1990) Evolution of the Central Tertiary Basin of Spitsbergen: towards a synthesis of sediment and plate tectonic history. *Palaeogeography, Palaeoclimatology, Palaeoecology* **80**, 153–72. doi: [10.1016/0031-0182\(90\)90127-S](https://doi.org/10.1016/0031-0182(90)90127-S).
- Ditchfield PW** (1997) High northern palaeolatitudes Jurassic–Cretaceous palaeotemperature variation: new data from Kong Karls Land, Svalbard. *Palaeogeography, Palaeoclimatology, Palaeoecology* **130**, 163–75. doi: [10.1016/S0031-0182\(96\)00054-5](https://doi.org/10.1016/S0031-0182(96)00054-5).
- Dörhöfer G and Davies EH** (1980) *Evolution of Archeopyle and Tabulation in Rhaetogonyaulacinean Dinoflagellate Cysts*. Life Sciences Miscellaneous Publication. Toronto, Canada: Royal Ontario Museum, 91 pp.
- Dörr N, Lisker F, Clift PD, Carter A, Gee DG, Tebenkov AM and Spiegel C** (2012) Late Mesozoic–Cenozoic exhumation history of northern Svalbard and its regional significance: constraints from apatite fission track analysis. *Tectonophysics* **514–517**, 81–92. doi: [10.1016/j.tecto.2011.10.007](https://doi.org/10.1016/j.tecto.2011.10.007).
- Duxbury S** (1977) A palynostratigraphy of the Berriasian to Barremian of the Speeton Clay of Speeton, England. *Palaeontographica Abteilung B* **160**, 17–67.
- Duxbury S** (1980) Barremian phytoplankton from Speeton, east Yorkshire. *Palaeontographica Abteilung B* **173**, 107–46.
- Duxbury S** (2001) A palynological zonation scheme for the Lower Cretaceous – United Kingdom sector, central North Sea. *Neues Jahrbuch fuer Geologie und Palaeontologie Abhandlungen* **219**, 95–137.
- Dypvik H, Eikeland TA, Backer-Owe K, Andresen A, Johansen H, Nagy EJ, Haremo P and Bjerke T** (1991) The Janusfjellet Subgroup (Bathonian to Hauterivian) on central Spitsbergen: a revised lithostratigraphy. *Polar Research* **9**, 21–44.
- Dypvik H, Nagy J and Krinsley DH** (1992) Origin of the Myklegardfjellet Bed, a basal Cretaceous marker on Spitsbergen. *Polar Research* **11**, 21–31.
- Erbacher J, Thurow J and Littke R** (1996) Evolution patterns of Radiolaria and organic matter variations: a new approach to identify sea-level changes in mid-Cretaceous pelagic environments. *Geology* **24**, 499–502. doi: [10.1130/0091-7613\(1996\)024<0499:EPORAO>2.3.CO;2](https://doi.org/10.1130/0091-7613(1996)024<0499:EPORAO>2.3.CO;2).
- Galloway JM, Tullius DN, Evenchick CA, Swindles GT, Hadlari T and Embry A** (2015) Early Cretaceous vegetation and climate change at high latitude: palynological evidence from Isachsen Formation, Arctic Canada. *Cretaceous Research* **56**, 399–420. doi: [10.1016/j.cretres.2015.04.002](https://doi.org/10.1016/j.cretres.2015.04.002).
- Gjelberg J and Steel RJ** (1995) Helvetiafjellet formation (Barremian–Aptian), Spitsbergen: characteristics of a transgressive succession. In *Sequence Stratigraphy on the Northwest European Margin* (eds RJ Steel, VL Felt, EP Johannessen and C Mathieu), pp. 571–93. Norwegian Petroleum Society Special Publications 5. doi: [10.1016/S0928-8937\(06\)80087-1](https://doi.org/10.1016/S0928-8937(06)80087-1).
- Gocht H** (1957) Mikroplankton aus dem nordwestdeutschen Neokom (Teil I). *Paläontologische Zeitschrift* **31**, 163–85.
- Gradstein FM, Kaminski MA and Agterberg FP** (1999) Biostratigraphy and paleoceanography of the Cretaceous seaway between Norway and Greenland. *Earth-Science Reviews* **46**, 27–98. doi: [10.1016/S0012-8252\(99\)00018-5](https://doi.org/10.1016/S0012-8252(99)00018-5).
- Grosfeld K** (1991) Palynological age constraints on the base of the Helvetiafjellet Formation (Barremian) on Spitsbergen. *Polar Research* **11**, 11–19.
- Grundvåg S-A, Jelby ME, Śliwińska KK, Nøhr-Hansen H, Aadland T, Sandvik SE, Tennvassås I, Engen T and Olausen S** (2019) Sedimentology and palynology of the Lower Cretaceous succession of central Spitsbergen: integration of subsurface and outcrop data. *Norwegian Journal of Geology* **99**, 1–32. doi: [10.17850/njg006](https://doi.org/10.17850/njg006).
- Grundvåg S-A, Marin D, Kairanov B, Śliwińska KK, Nøhr-Hansen H, Jelby ME, Escalona A and Olausen S** (2017) The Lower Cretaceous succession of the northwestern Barents Shelf: onshore and offshore correlations. *Marine and Petroleum Geology* **86**, 834–57. doi: [10.1016/j.marpetgeo.2017.06.036](https://doi.org/10.1016/j.marpetgeo.2017.06.036).
- Grundvåg S-A and Olausen S** (2017) Sedimentology of the Lower Cretaceous at Kikutodden and Keilhauffjellet, southern Spitsbergen: implications for an onshore-offshore link. *Polar Research* **36**, 1302124. doi: [10.1080/17518369.2017.1302124](https://doi.org/10.1080/17518369.2017.1302124).
- Hammer Ø, Alsen P, Grundvåg S-A, Jelby ME, Nøhr-Hansen H, Olausen S, Senger K, Śliwińska KK and Smelror M** (2018) Comment on “Redox conditions, productivity, and volcanic input during deposition of uppermost Jurassic and Lower Cretaceous organic-rich siltstones in Spitsbergen, Norway” by Rakocinski *et al.* (2018). *Cretaceous Research* **96**, 241–3. doi: [10.1016/j.cretres.2018.02.014](https://doi.org/10.1016/j.cretres.2018.02.014).
- Harland WB** (1997) *The Geology of Svalbard*. Geological Society of London, Memoir no. 17. London: The Geological Society, 521 pp.
- Heilmann-Clausen C** (1987) Lower Cretaceous dinoflagellate biostratigraphy in the Danish Central Trough. *Danmarks Geologiske Undersøgelse, Series A*, **17**, 1–89.
- Helby R** (1987) *Muderongia* and related dinoflagellates of the latest Jurassic to Early Cretaceous of Australasia. In *Studies in Australian Mesozoic Palynology* (ed. PA Jell), pp. 297–336. Sydney: Association of Australian Palaeontologists.
- Henriksen E, Ryseth AE, Larssen GB, Heide T, Rønning K, Sollid K and Stoupakova AV** (2011) Chapter 10 Tectonostratigraphy of the greater Barents Sea: implications for petroleum systems. In *Arctic Petroleum Geology* (eds AM Spencer, AFE Embry, DL Gautier, AV Stoupakova and K Sørensen), pp. 163–95. Geological Society of London, Memoirs no. 35. doi: [10.1144/M35.10](https://doi.org/10.1144/M35.10).
- Herrle JO, Schröder-Adams CJ, Davis W, Pugh AT, Galloway JM and Fath J** (2015) Mid-Cretaceous High Arctic stratigraphy, climate, and Oceanic Anoxic Events. *Geology* **43**, 403–6. doi: [10.1130/G36439.1](https://doi.org/10.1130/G36439.1).
- Hochuli PA, Menegatti AP, Weissert H, Riva A, Erba E and Premoli Silva I** (1999) Episodes of high productivity and cooling in the early Aptian Alpine Tethys. *Geology* **27**, 657–60. doi: [10.1130/0091-7613\(1999\)027<0657:EOHPAC>2.3.CO;2](https://doi.org/10.1130/0091-7613(1999)027<0657:EOHPAC>2.3.CO;2).
- Holden JC** (1970) Reconstruction of Pangaea: breakup and dispersion of continents, Permian to Present. *Journal of Geographical Research* **75**, 4939–56. doi: [10.1029/JB075i026p04939](https://doi.org/10.1029/JB075i026p04939).
- Huber BT, MacLeod G, Watkins DK and Coffin MF** (2018) The rise and fall of the Cretaceous Hot Greenhouse climate. *Global and Planetary Change* **167**, 1–23. doi: [10.1016/j.gloplacha.2018.04.004](https://doi.org/10.1016/j.gloplacha.2018.04.004).

- Hurum JH, Druckenmiller PS, Hammer Ø, Nakrem HA and Olausen S (2016a) The theropod that wasn't: an ornithomimid tracksite from the Helvetiafjellet Formation (Lower Cretaceous) of Boltodden, Svalbard. In *Mesozoic Biotas of Scandinavia and its Arctic Territories* (eds BP Kear, J Lindren, JH Hurum, J Milàn and V Vajda), pp. 189–206. Geological Society of London, Special Publication no. 434. doi: [10.1144/sp434.10](https://doi.org/10.1144/sp434.10).
- Hurum JH, Roberts AJ, Dyke GJ, Grundvåg S-A, Nakrem HA, Midtkandal I, Śliwińska KK and Olausen S (2016b) Bird or maniraptoran dinosaur? A femur from the Albian strata of Spitsbergen. *Palaeontologia Polonica* **67**, 137–47. doi: [10.4202/pp.2016.67_137](https://doi.org/10.4202/pp.2016.67_137).
- Ioannides NS, Stavrinou GN and Downie C (1977) Kimmeridgian microplankton from Clavell's Hard, Dorset, England. *Micropaleontology* **22**, 443–78.
- Jain KP and Millepieud P (1973) Cretaceous microplankton from Senegal Basin, NW Africa. 1. Some new genera, species and combinations of dinoflagellates. *The Palaeobotanist* **20**, 22–32.
- Jelby ME, Grundvåg S-A, Helland-Hansen W, Olausen S and Stemmerik L (2020) Tempestite facies variability and storm-depositional processes across a wide ramp: Towards a polygenetic model for hummocky cross-stratification. *Sedimentology* **67**, 742–81. doi: [10.1111/sed.12671](https://doi.org/10.1111/sed.12671).
- Jenkyns HC (2010) Geochemistry of oceanic anoxic events. *Geochemistry, Geophysics, Geosystems* **11**, 1–30. doi: [10.1029/2009GC002788](https://doi.org/10.1029/2009GC002788).
- Jenkyns HC, Schouten-Huibers L, Schouten S and Sinninghe Damsté JS (2012) Warm Middle Jurassic–Early Cretaceous high-latitude sea-surface temperatures from the Southern Ocean. *Climate of the Past* **8**, 215–26. doi: [10.5194/cp-8-215-2012](https://doi.org/10.5194/cp-8-215-2012).
- Johanson FKB, Turchyn AV and Edmonds M (2011) Decarbonation efficiency in subduction zones: implications for warm Cretaceous climates. *Earth and Planetary Science Letters* **303**, 143–52. doi: [10.1016/j.epsl.2010.12.049](https://doi.org/10.1016/j.epsl.2010.12.049).
- Kairanov B, Escalona A, Mordasova A, Śliwińska K and Suslova A (2018) Lower Cretaceous tectonostratigraphic evolution of the north central Barents Sea. *Journal of Geodynamics* **119**, 183–98. doi: [10.1016/j.jog.2018.02.009](https://doi.org/10.1016/j.jog.2018.02.009).
- Koevoets MJ, Hammer Ø, Olausen S, Senger K and Smelror M (2018) Integrating subsurface and outcrop data of the middle Jurassic to lower Cretaceous Agardhfjellet Formation in central Spitsbergen. *Norsk Geologisk Tidsskrift* **98**, 1–34. doi: [10.17850/njg98-4-01](https://doi.org/10.17850/njg98-4-01).
- Koopmann H, Schreckenberger B, Franke D, Becker K and Schnabel M (2014) The late rifting phase and continental break-up of the southern South Atlantic: the mode and timing of volcanic rifting and formation of earliest oceanic crust. In *Magmatic Rifting and Active Volcanism* (eds TJ Wright, A Ayele, DJ Ferguson, T Kidane and C Vye-Brown), pp. 315–40. Geological Society of London, Special Publication no. 420. doi: [10.1144/sp420.2](https://doi.org/10.1144/sp420.2).
- Lebedeva NK and Nikitenko BL (1999) Dinoflagellate cysts and microforaminifera of the Lower Cretaceous Yatria River section, subarctic Ural, NW Siberia (Russia). Biostratigraphy, palaeoenvironmental and palaeogeographic discussion. *Grana* **38**, 134–43. doi: [10.1080/00173139908559222](https://doi.org/10.1080/00173139908559222).
- Leckie RM, Bralower TJ and Cashman R (2002) Oceanic anoxic events and plankton evolution: Biotic response to tectonic forcing during the mid-Cretaceous. *Paleoceanography* **17**, 13 doi: [10.1029/2001PA000623](https://doi.org/10.1029/2001PA000623).
- Lehmann J (2015) Ammonoid biostratigraphy of the Cretaceous—an overview. In *Ammonoid Paleobiology: From Macroevolution to Paleogeography* (eds C Klug, D Korn, K De Baets, I Kruta and RH Mapes), pp. 403–29. Dordrecht: Springer. doi: [10.1007/978-94-017-9633-0](https://doi.org/10.1007/978-94-017-9633-0).
- Littler K, Robinson SA, Bown PR, Nederbragt AJ and Pancost RD (2011) High sea-surface temperatures during the Early Cretaceous Epoch. *Nature Geoscience* **4**, 169–72. doi: [10.1038/ngeo1081](https://doi.org/10.1038/ngeo1081).
- Lofaldi M and Thusu B (1976) Microfossils from the Janusfjellet Subgroup (Jurassic–Lower Cretaceous) at Agardhfjellet and Keilhaufjellet, Spitsbergen. A preliminary report. *Norsk Polarinstitutt Årbok* **1975**, 69–77.
- Marin D, Escalona A, Grundvåg SA, Nøhr-Hansen H and Kairanov B (2018a) Effects of adjacent fault systems on drainage patterns and evolution of uplifted rift shoulders: the Lower Cretaceous in the Loppa High, southwestern Barents Sea. *Marine and Petroleum Geology* **94**, 212–29. doi: [10.1016/j.marpetgeo.2018.04.009](https://doi.org/10.1016/j.marpetgeo.2018.04.009).
- Marin D, Escalona A, Grundvåg SA, Olausen S, Sandvik S and Śliwińska KK (2018b) Unravelling key controls on the rift climax to post-rift fill of marine rift basins: insights from 3D seismic analysis of the Lower Cretaceous of the Hammerfest Basin, SW Barents Sea. *Basin Research* **30**, 587–612. doi: [10.1111/bre.12266](https://doi.org/10.1111/bre.12266).
- Marin D, Escalona A, Śliwińska KK, Nøhr-Hansen H and Mordasova A (2017) Sequence stratigraphy and lateral variability of Lower Cretaceous clinofolds in the southwestern Barents Sea. *American Association of Petroleum Geologists Bulletin* **101**, 1487–517. doi: [10.1306/10241616010](https://doi.org/10.1306/10241616010).
- McIntyre DJ and Brideaux WW (1980) Valanginian miospore and microplankton assemblages from the northern Richardson Mountains, District of Mackenzie. *Geological Survey of Canada, Bulletin* **320**, 1–57.
- Midtkandal I and Nystuen JP (2009) Depositional architecture of a low-gradient ramp shelf in an epicontinental sea: the lower Cretaceous of Svalbard. *Basin Research* **21**, 655–75. doi: [10.1111/j.1365-2117.2009.00399.x](https://doi.org/10.1111/j.1365-2117.2009.00399.x).
- Midtkandal I, Nystuen JP and Nagy J (2007) Paralic sedimentation on an epicontinental ramp shelf during a full cycle of relative sea-level fluctuation; the Helvetiafjellet Formation in Nordenskiöld land, Spitsbergen. *Norsk Geologisk Tidsskrift* **87**, 343–59.
- Midtkandal I, Nystuen JP, Nagy J and Mørk A (2008) Lower Cretaceous lithostratigraphy across a regional subaerial unconformity in Spitsbergen: the Rurikfjellet and Helvetiafjellet Formations. *Norsk Geologisk Tidsskrift* **88**, 287–304.
- Midtkandal I, Svensen HH, Planke S, Corfu F, Polteau S, Torsvik TH, Faleide JJ, Grundvåg SA, Selnes H, Kürschner W and Olausen S (2016) The Aptian (Early Cretaceous) oceanic anoxic event (OAE1a) in Svalbard, Barents Sea, and the absolute age of the Barremian–Aptian boundary. *Palaeogeography, Palaeoclimatology, Palaeoecology* **463**, 126–35. doi: [10.1016/j.palaeo.2016.09.023](https://doi.org/10.1016/j.palaeo.2016.09.023).
- Mutterlose J, Pauly S and Steuber T (2009) Temperature controlled deposition of early Cretaceous (Barremian–early Aptian) black shales in an epicontinental sea. *Palaeogeography, Palaeoclimatology, Palaeoecology* **273**, 330–45 doi: [10.1016/j.palaeo.2008.04.026](https://doi.org/10.1016/j.palaeo.2008.04.026).
- Nikitenko BL, Pestchevitskaya EB, Lebedeva NK and Ilyina VI (2008) Micropalaeontological and palynological analyses across the Jurassic–Cretaceous boundary on Nordvik Peninsula, Northeast Siberia. *Newsletters on Stratigraphy* **42**, 181–222. doi: [10.1127/0078-0421/2008/0042-0181](https://doi.org/10.1127/0078-0421/2008/0042-0181).
- Nøhr-Hansen H (1993) *Dinoflagellate Cyst Stratigraphy of the Barremian to Albian, Lower Cretaceous, North-East Greenland*. Danmarks: Grønlands Geologiske Undersøgelse, 166 pp.
- Nøhr-Hansen H and McIntyre DJ (1998) Upper Barremian to upper Albian (Lower Cretaceous) dinoflagellate cyst assemblages, Canadian Arctic archipelago. *Palynology* **22**, 143–66. doi: [10.1080/01916122.1998.9989506](https://doi.org/10.1080/01916122.1998.9989506).
- Nøhr-Hansen H, Piasecki S and Alsen P (2019) A Cretaceous dinoflagellate cyst zonation for NE Greenland. *Geological Magazine*, published online 29 October 2019. doi: [10.1017/S0016756819001043](https://doi.org/10.1017/S0016756819001043).
- Norris G (1978) Phylogeny and a revised supra-generic classification for Triassic–Quaternary organic-walled dinoflagellate cysts (Pyrrhophyta). Part II. Families and sub-orders of fossil dinoflagellates. *Neues Jahrbuch für Geologie und Paläontologie, Abhandlungen* **156**, 1–30.
- O'Brien CL, Robinson SA, Pancost RD, Sinninghe Damsté JS, Schouten S, Lunt DJ, Alsenz H, Bornemann A, Bottini C, Brassell SC, Farnsworth A, Forster A, Huber BT, Inglis GN, Jenkyns HC, Linnert C, Littler K, Markwick P, McAnena A, Mutterlose J, Naafs BDA, Püttmann W, Sluijs A, van Helmond NAGM, Vellekoop J, Wagner T and Wrobel NE (2017) Cretaceous sea-surface temperature evolution: constraints from TEX₈₆ and planktonic foraminiferal oxygen isotopes. *Earth-Science Reviews* **172**, 224–47. doi: [10.1016/j.earscirev.2017.07.012](https://doi.org/10.1016/j.earscirev.2017.07.012).
- Ogg JG, Hinnov LA and Huang C (2012) Cretaceous. In *The Geologic Time Scale 2012* (eds FM Gradstein, JG Ogg, M Schmitz and G Ogg), pp. 793–853. Amsterdam: Elsevier. doi: [10.1016/B978-0-444-59425-9.00027-5](https://doi.org/10.1016/B978-0-444-59425-9.00027-5).
- Ogg JG, Ogg GM and Gradstein FM (2016) 13 - Cretaceous. In *A Concise Geologic Time Scale 2016* (eds JG Ogg, GM Ogg and FM Gradstein), pp. 167–86. Amsterdam: Elsevier, doi: [10.1016/B978-0-444-59467-9.00013-3](https://doi.org/10.1016/B978-0-444-59467-9.00013-3).

- Parker JR** (1967) The Jurassic and Cretaceous Sequence in Spitsbergen. *Geological Magazine* **104**, 487–505. doi: [10.1017/S0016756800049220](https://doi.org/10.1017/S0016756800049220).
- Pedersen GK and Nøhr-Hansen H** (2014) Sedimentary successions and palynoevent stratigraphy from the non-marine Lower Cretaceous to the marine Upper Cretaceous of the Nuussuaq Basin, West Greenland. *Bulletin of Canadian Petroleum Geology* **64**, 261–88. doi: [10.2113/gscpgbull.62.4.261](https://doi.org/10.2113/gscpgbull.62.4.261).
- Pestchevitskaya EB** (2007) Dinocyst biostratigraphy of the Lower Cretaceous in North Siberia. *Stratigraphy and Geological Correlation* **15**, 577–609. doi: [10.1134/s0869593807060020](https://doi.org/10.1134/s0869593807060020).
- Pestchevitskaya E, Lebedeva N and Ryabokon A** (2011) Uppermost Jurassic and lowermost Cretaceous dinocyst successions of Siberia, the Subarctic Urals and Russian platform and their interregional correlation. *Geologica Carpathica* **62**, 189–202. doi: [10.2478/v10096-011-0016-9](https://doi.org/10.2478/v10096-011-0016-9).
- Piasecki S** (1979) Hauterivian dinoflagellate cysts from Milne Land, East Greenland. *Bulletin of the Geological Society of Denmark* **28**, 31–7.
- Piasecki S, Nøhr-Hansen H and Dalhoff F** (2018) Revised stratigraphy of Kap Rigsdagen beds, Wandel Sea Basin, North Greenland. *Newsletters on Stratigraphy* **51**, 411–25. doi: [10.1127/nos/2018/0444](https://doi.org/10.1127/nos/2018/0444).
- Pocock SAJ** (1976) A preliminary dinoflagellate zonation of the uppermost Jurassic and lower part of the Cretaceous, Canadian Arctic, and possible correlation in the Western Canada Basin. *Journal of Geoscience and Man* **7**, 101–14. doi: [10.2307/3687262](https://doi.org/10.2307/3687262).
- Polteau S, Hendriks BWH, Planke S, Ganerød M, Corfu F, Faleide JJ, Midtkandal I, Svensen HS and Myklebust R** (2016) The Early Cretaceous Barents Sea Sill Complex: distribution, $^{40}\text{Ar}/^{39}\text{Ar}$ geochronology, and implications for carbon gas formation. *Palaeogeography, Palaeoclimatology, Palaeoecology* **441**, 83–95. doi: [10.1016/j.palaeo.2015.07.007](https://doi.org/10.1016/j.palaeo.2015.07.007).
- Price GD and Passey BH** (2013) Dynamic polar climates in a greenhouse world: evidence from clumped isotope thermometry of Early Cretaceous belemnites. *Geology* **41**, 923–6. doi: [10.1130/G34484.1](https://doi.org/10.1130/G34484.1).
- Prössl KF** (1990) Dinoflagellaten der Kreide – Unter-Hauterive bis Ober-Turon – im niedersächsischen Becken. Stratigraphie und Fazies in der Kernbohrung Konrad 101 sowie einiger anderer Bohrungen in Nordwestdeutschland. *Palaeontographica Abteilung B* **218**, 93–191.
- Rakociński M, Zatoń M, Marynowski L, Gedl P and Lehmann J** (2018) Redox conditions, productivity, and volcanic input during deposition of uppermost Jurassic and Lower Cretaceous organic-rich siltstones in Spitsbergen, Norway. *Cretaceous Research* **89**, 126–47. doi: [10.1016/j.cretres.2018.02.014](https://doi.org/10.1016/j.cretres.2018.02.014).
- Riding JB, Fedorova VA and Ilyina VI** (1999) Jurassic and lowermost Cretaceous dinoflagellate cyst biostratigraphy of the Russian Platform and Northern Siberia, Russia. *American Association of Stratigraphic Palynologists Contribution Series* **36**, 1–184.
- Riding JB and Fensome RA** (2003) A review of *Scriniodinium* Klement 1957, *Endoscrinium* (Klement 1960) Vozzhennikova 1967 and related dinoflagellate cyst taxa. *Palynology* **26**, 5–33.
- Rogers JJW and Santosh M** (2004) Continents and supercontinents. *Gondwana Research* **7**, 653. doi: [10.1016/S1342-937X\(05\)70827-3](https://doi.org/10.1016/S1342-937X(05)70827-3).
- Sarjeant WAS** (1966) Further dinoflagellate cysts from the Speeton Clay. In *Studies on Mesozoic and Cainozoic Dinoflagellate Cysts* (eds RJ Davey, C Downie, WAS Sarjeant and GL Williams), pp. 199–214. London: British Museum (Natural History) Geology, Bulletin, Supplement 3.
- Scotese C** (2014) *Atlas of Early Cretaceous Paleogeographic Maps, PALEOMAP Atlas for ArcGIS, volume 2, The Cretaceous, Maps 23–31, Mollweide Projection*. Evanston, IL: PALEOMAP Project. doi: [10.13140/2.1.4099.4560](https://doi.org/10.13140/2.1.4099.4560).
- Senger K, Tveranger J, Ogata K, Braathen A and Planke S** (2014) Late Mesozoic magmatism in Svalbard: a review. *Earth-Science Reviews* **139**, 123–44. doi: [10.1016/j.earscirev.2014.09.002](https://doi.org/10.1016/j.earscirev.2014.09.002).
- Śliwińska KK** (2019) Early Oligocene dinocysts as a tool for palaeoenvironment reconstruction and stratigraphical framework – a case study from a North Sea well. *Journal of Micropalaeontology* **38**, 143–76. doi: [10.5194/jm-38-143-2019](https://doi.org/10.5194/jm-38-143-2019).
- Smelror M** (1986) Jurassic and Lower Cretaceous palynomorph assemblages from Cape Flora, Franz Josef Land, Arctic USSR. *Norsk Geologisk Tidsskrift* **66**, 107–19.
- Smelror M and Dypvik H** (2005) Marine microplankton biostratigraphy of the Volgian–Ryazanian boundary strata, western Barents Shelf. *Norges geologiske undersøkelse Bulletin* **443**, 61–9.
- Smelror M and Dypvik H** (2006) The sweet aftermath: environmental changes and biotic restoration following the marine Mjøltnir impact (Volgian–Ryazanian Boundary, Barents Shelf). In *Biological Processes Associated with Impact Events* (eds C Cockell, C Koeberl and I Gilmour), pp. 143–78. Berlin: Springer-Verlag. doi: [10.1007/3-540-25736-5_7](https://doi.org/10.1007/3-540-25736-5_7).
- Smelror M and Larssen GB** (2016) Are there Upper Cretaceous sedimentary rocks preserved on Sørkapp land, Svalbard?. *Norsk Geologisk Tidsskrift* **96**, 1–12. doi: [10.17850/njg96-2-05](https://doi.org/10.17850/njg96-2-05).
- Smelror M, Larssen GB, Olaussen S, Rømuld A and Williams R** (2018) Late Triassic to Early Cretaceous palynostratigraphy of Kong Karls Land, Svalbard, Arctic Norway, with correlations to Franz Josef Land, Arctic Russia. *Norwegian Journal of Geology* **98**, 1–31. doi: [10.17850/njg98-4-04](https://doi.org/10.17850/njg98-4-04).
- Smelror M, Mørk A, Monteil E, Rutledge D and Leereveld H** (1998) The Klippfisk Formation – a new lithostratigraphic unit of Lower Cretaceous platform carbonates on the Western Barents Shelf. *Polar Research* **17**, 181–202. doi: [10.1111/j.1751-8369.1998.tb00271.x](https://doi.org/10.1111/j.1751-8369.1998.tb00271.x).
- Smelror M, Petrov OV, Larssen GB and Werner SC** (eds) (2009) *Geological History of the Barents Sea*. Trondheim: Norges geologiske undersøkelse/ Geological Survey of Norway. Available at: https://issuu.com/ngu/docs/atlas_-_geological_history_of_the_b/1?e=3609664/9026048.
- Thusu B** (1978) Aptian to Toarcian dinoflagellate cysts from Arctic Norway. In *Distribution of Biostratigraphically Diagnostic Dinoflagellate Cysts and Miospore from Northwest European Continental Shelf and Adjacent Areas* (ed. B Thusu), pp. 61–95. London: Continental Shelf Institute Publication 100.
- Torsvik TH, Carlos D, Mosar J, Cocks LRM and Malme T** (2002) Global reconstructions and North Atlantic paleogeography 440 Ma to Recent. In *BATLAS – Mid Norway Plate Reconstruction Atlas with Global and Atlantic Perspectives* (coord. EA Eide), pp. 18–39. Trondheim: NGU.
- Trabucho Alexandre J, Tuenter E, Henstra GA, van der Zwan KJ, van de Wal RSW, Dijkstra HA and de Boer PL** (2010) The mid-Cretaceous North Atlantic nutrient trap: black shales and OAEs. *Paleoceanography and Paleoclimatology* **25**, PA4201. doi: [10.1029/2010PA001925](https://doi.org/10.1029/2010PA001925).
- van Hinsbergen DJJ, de Groot LV, van Schaik SJ, Spakman W, Bijl PK, Sluijs A, Langereis CG and Brinkhuis H** (2015) A paleolatitude calculator for paleoclimate studies. *PLoS ONE* **10**, e0126946. doi: [10.1371/journal.pone.0126946](https://doi.org/10.1371/journal.pone.0126946).
- Vickers ML, Price GD, Jerrett RM and Watkinson M** (2016) Stratigraphic and geochemical expression of Barremian–Aptian global climate change in Arctic Svalbard. *Geosphere* **12**, 1594–605. doi: [10.1130/GES01344.1](https://doi.org/10.1130/GES01344.1).
- Vozzhennikova TF** (1967) *Iskopaemye Peridinei Yurskikh, Melovykh i Paleogenovykh Otlozheniy SSSR*. Moscow: Izdatelstvo Nauka.
- Wierzbowski A, Hryniewicz K, Hammer Ø, Nakrem HA and Little CTS** (2011) Ammonites from hydrocarbon seep carbonate bodies from the uppermost Jurassic – lowermost Cretaceous of Spitsbergen and their biostratigraphical importance. *Neues Jahrbuch für Geologie und Paläontologie – Abhandlungen* **262**, 267–88. doi: [10.1127/0077-7749/2011/0198](https://doi.org/10.1127/0077-7749/2011/0198).
- Wiggins VD** (1972) Two new Lower Cretaceous dinoflagellate genera from southern Alaska (U.S.A.). *Review of Palaeobotany and Palynology* **14**, 297–308.
- White HH** (1842) On fossil *Xanthidia*. *Microscopical Journal, London* **11**, 35–40.
- Williams GL and Fensome RA** (2016) Fossil dinoflagellates: nomenclatural proposals in anticipation of a revised DINOFLAJ database. *Palynology* **40**, 137–43.
- Williams G, Fensome R and MacRae R** (2017) The Lentins and Williams Index of fossil dinoflagellates 2017 edition. *American Association of Stratigraphic Palynologists Contribution Series* **48**, 1–1097.
- Zakharov VA** (1987) The bivalve *Buchia* and the Jurassic–Cretaceous boundary in the Boreal province. *Cretaceous Research* **8**, 141–53. doi: [10.1016/0195-6671\(87\)90018-8](https://doi.org/10.1016/0195-6671(87)90018-8).

Appendix 1. Taxonomic notes on characteristic dinocyst taxa of the Rurikfjellet and Helvetiafjellet formations

Appendix 1a. Stratigraphic range of *Endoscrinium hauterivianum* (Duxbury, 2001) Riding & Fensome, 2003

Figure 3o, p

1978 *Apteodinium* sp. A (Bjærke, 1978)

1980? *Apteodinium* sp. A of Bjærke (1978) Bjærke plate X, figs 1, 2

1991 *Apteodinium* sp. A of Bjærke (1978) Grøsfjeld plate 4, figs D–F

2001 *Scriniodinium hauterivianum* Duxbury, 2001

2003 *Endoscrinium hauterivianum* (Duxbury, 2001) Riding & Fensome

The holotype of *E. hauterivianum* was described from the UK sector of the North Sea Basin (Duxbury, 2001). The taxon was described as restricted to the Hauterivian with the LO within the lowermost upper Hauterivian (Duxbury, 2001). We here suggest that *Apteodinium* sp. A of Bjærke (1978), which was recorded in the Valanginian to Hauterivian succession of the Rurikfjellet Formation (T. Bjærke, unpub. report, 1980), is a synonym of *E. hauterivianum*. Grøsfjeld (1991) noted that the species was present in numerous locations on Spitsbergen and can be used as a Hauterivian marker in the region. However, she also pointed out that at Janusfjellet the LO of *Apteodinium* sp. A of Bjærke (1978) post-dates the LO of *N. kostromiensis* (for the stratigraphic range of *N. kostromiensis* see Appendix 1e) and thus it may range into the Barremian. Grøsfjeld (1991) did not observe *N. kostromiensis* in the Bohemanflya outcrop section (see fig. 6 in Grøsfjeld, 1991), only *N. pannosa* (see below) and *Apteodinium* sp. A of Bjærke (1978).

Spitsbergen – this study. In the present study *E. hauterivianum* is recorded in all studied sections. We apply the FO of *E. hauterivianum* as a marker for the base Hauterivian and the LO as the marker for the earliest late Hauterivian. In the two sections with the highest dinocyst diversity and the greatest assemblage abundance (Bohemanflya, online Supplementary Material Fig. S1, Myklegardfjellet, online Supplementary Material Fig. S2, and Fig. 8), the LO of *E. hauterivianum* pre-dates the LO of *N. kostromiensis*. This is in contrast to the observations by Grøsfjeld (1991) from the Bohemanflya outcrop section. We speculate that the longer range of *N. kostromiensis* observed by us may be an effect of different sampling strategies carried out in both studies. In the studied material the taxon is rare to abundant (i.e. <1 % or >50 % of the total dinocyst assemblage).

Appendix 1b. LO of *Gochteodinia villosa* (Vozzhennikova, 1967) Norris, 1978

Figure 4a–c

G. villosa is divided into two subspecies, *G. villosa* subsp. *villosa* (Vozzhennikova, 1967) and *G. villosa* subsp. *multifurcata* (Davey, 1982). The stratigraphic ranges of these subspecies are different (Fig. 7). The FO of *G. villosa multifurcata* post-dates the FO of *G. villosa villosa*, and thus distinguishing the two subspecies is very useful for increasing the resolution of the age framework. In the North Sea Basin, *G. villosa multifurcata* ranges from the lower Valanginian (Heilmann-Clausen, 1987) to the lowermost Hauterivian (Heilmann-Clausen, 1987; Costa & Davey, 1992) or to the Valanginian–Hauterivian boundary (Davey, 1982; Bailey, 2019). The youngest LOs of *G. villosa villosa* are reported at the Ryazanian–Valanginian boundary (Heilmann-Clausen, 1987) or in the lowermost Valanginian (Costa & Davey, 1992; Bailey,

2019). Davey (1982) and Nøhr-Hansen *et al.* (2019) reported the youngest occurrence of the taxon in the upper Ryazanian – upper Berriasian from Denmark and NE Greenland, respectively. In the Sverdrup Basin, Arctic Canada, *G. villosa* (not differentiated into subspecies, and possibly *G. villosa multifurcata*) was found in the Valanginian (Davies, 1983). In the Barents Sea, (possibly reworked) specimens of *G. villosa* were reported in the assemblages referred to the Hauterivian – lower Barremian (Århus *et al.* 1990). Århus (1991) shows that on central Spitsbergen *G. villosa* occurs in the Valanginian and Hauterivian strata, while *G. villosa multifurcata* has a slightly shorter range: Valanginian to lowermost Hauterivian. In the Valanginian part of the succession both taxa are present consistently. In post-Valanginian strata both taxa occur only sporadically (fig. 13 in Århus, 1988), and thus their presence may be an effect of reworking.

Spitsbergen – this study. Specimens referred to *G. villosa villosa* and *G. villosa multifurcata* are slightly more elongate than the type material (cf. e.g. Davey, 1982). The poor preservation of some of the specimens encountered in the present study sometimes precludes an unambiguous separation of the two subspecies. We distinguish subspecies only if the determination is possible. In a few samples *G. villosa* makes up 2–4 % of the total dinocyst assemblage. Otherwise, the species occurs persistently in the lower part of the Rurikfjellet Formation (Myklegardfjellet, DH5R), but is rather rare.

Appendix 1c. Stratigraphic range and abundance interval of *Muderongia australis* Helby, 1987

Figure 4e

The youngest record on NE Greenland of the taxon is from the upper Hauterivian (Nøhr-Hansen, 1993; Nøhr-Hansen *et al.* 2019). In the other few existing studies, *M. australis* is reported either from the Hauterivian (Århus *et al.* 1990; Prössl, 1990) or from the Barremian (Helby, 1987; Davey, 1988). In Spitsbergen, *M. australis* is restricted to the upper part of the Rurikfjellet Formation (Århus *et al.* 1990). Århus *et al.* (1990) also noted an acme of *M. australis* in the interval referred to the Hauterivian – lower Barremian and mentioned that the *M. australis* acme may be related to the early Barremian flooding event.

Spitsbergen – this study. We observe the persistent occurrence of *M. australis* in the upper part of the Rurikfjellet Formation within all the studied sites. Thus, we confirm the observations of Århus *et al.* (1990). In the topmost sample from the Rurikfjellet Formation at the Myklegardfjellet outcrop, *M. australis* occurs as a local acme, which we interpret to be synchronous with the acme observed in the Barents Sea (Århus *et al.* 1990) and NE Greenland (Nøhr-Hansen, 1993).

Appendix 1d. *Muderongia extensiva* and *Muderongia tetracantha*

Figure 4d, g, h

In the North Sea Basin, the LO of *M. extensiva* is a well established earliest Hauterivian marker (Heilmann-Clausen, 1987; Costa & Davey, 1992; Duxbury, 2001). *M. tetracantha* has a slightly younger range, i.e. from the Hauterivian to the lowermost Barremian (Costa & Davey, 1992; Duxbury, 2001) or even Aptian (Heilmann-Clausen, 1987; Nøhr-Hansen, 1993; Nøhr-Hansen & McIntyre, 1998). Notably, some authors merge *M. tetracantha* with *Muderongia crucis* (Costa & Davey, 1992; Bailey, 2019) or consider *M. crucis* as a junior synonym (e.g. Helby, 1987). Nevertheless, *M. tetracantha* is considered the most typical taxon for Hauterivian – lower Barremian strata (see discussion in

Heilmann-Clausen, 1987). More details concerning the stratigraphic ranges of these two taxa in the Boreal and the European Boreal realm is shown in Figure 7.

The differences in morphologies of *M. tetracantha* and *M. extensiva* are distinctive. The lateral horns of *M. extensiva* are long and extend almost at right angles from the tests (Duxbury, 1977), while in *M. tetracantha* the horns bend downwards (Gocht, 1957). Furthermore, *M. extensiva* in contrast to *M. tetracantha* show a distinct plate differentiation at the lateral edge (Helby, 1987).

Spitsbergen – this study. In the material encountered in the present study we observe transitional forms between *M. extensiva* and *M. tetracantha*. Some of these forms resemble *M. tetracantha* in their general outline, but on one or both lateral horns, we observe a distinct plate differentiation, a feature typical for *M. extensiva* (Fig. 4g). We observe the earliest record of *M. tetracantha* below the FO of *E. hauerivianum* (online Supplementary Material Fig. S1), but in sections with high dinocyst diversity and high relative abundance, the FO of *M. tetracantha* is observed within the range of *E. hauerivianum* (online Supplementary Material Figs S1, S2, S6, and Fig. 4)

Appendix 1e. Stratigraphic range of *Nelchinopsis kostromiensis* (Vozzhennikova, 1967) Wiggins, 1972

Figure 4m, n

In the majority of existing studies of the North Sea Basin (Fig. 7), the range of this species is limited to the upper lower Valanginian – upper Hauterivian (Costa & Davey, 1992; Duxbury, 2001) or to the Hauterivian (Davey, 1982; Heilmann-Clausen, 1987). In NE Greenland the taxon first occurs in the middle upper Valanginian and is not observed above the lower to upper Hauterivian *N. kostromiensis* Subzone (Nøhr-Hansen, 1993; Nøhr-Hansen *et al.* 2019). Some studies report the FO of *N. kostromiensis* as early as at the lower–upper Valanginian boundary (Costa & Davey, 1992) and its LO in the lowermost Barremian (Bailey, 2019). However, the Hauterivian–Barremian boundary in Bailey (2019) is dated as 130 Ma, so it is slightly younger than in the Geological Time Scale 2016 where it is dated as 130.8 Ma (Ogg *et al.* 2016). In the Svedrup Basin, Arctic Canada, *N. kostromiensis* was observed together with *Gochteodinia villosa* in the middle-upper upper Valanginian succession (Davies, 1983). In some older studies *N. kostromiensis* was reported from the lowermost Barremian (Heilmann-Clausen, 1987; Smelror *et al.* 1998), from the *Simbirskites variabilis* ammonite zone. Today, the zone is considered to be Hauterivian (Ogg *et al.* 2016).

Spitsbergen – this study. The FO and LO of *N. kostromiensis* are important stratigraphic events within the Rurikfjellet Formation. The range of *N. kostromiensis* virtually spans the entire unit at the three outcrops and in the DH5R core. Applying the age constraint based on the LOs of *Tubotuberella apatela* and *Gochteodinia villosa villosa*, the FO of *Nelchinopsis kostromiensis* in Spitsbergen is considered as an early Valanginian event, observed in the lower part of the Rurikfjellet Formation. The LO of *N. kostromiensis* is observed in the upper part of the Rurikfjellet Formation and is probably of latest Hauterivian – earliest Barremian age.

Appendix 1f. FO of *Odontochitina nuda* (Gocht, 1957) Dörhöfer & Davies, 1980

Figure 5e

The holotype of *O. nuda* was described from the upper Hauterivian (Gocht, 1957). Other studies from Europe and

Canada also suggest a Hauterivian to Barremian stratigraphic range for the taxon (see discussion in Nøhr-Hansen, 1993) (Fig. 7). In NE Greenland, *O. nuda* is restricted to the uppermost lower Barremian to lower Aptian (Nøhr-Hansen, 1993). In the Barents Sea, the taxon was reported from lower Barremian strata by Århus (in Århus *et al.* 1990), but notably this study was carried out only on a Berriasian to lower Barremian succession. Therefore, the youngest occurrence of the taxon in the Barents Sea is unknown.

Spitsbergen – this study. *O. nuda* is restricted to the Helvetiafjellet Formation. The FO is observed within the middle (the DH2 core) or the upper (the Ullaberget outcrop section) part of the formation. The most probable time span for the taxon in Spitsbergen is Barremian to early Aptian.

Appendix 1g. FO of *Oligosphaeridium abaculum* Davey, 1979b

Figure 5f

The holotype of *O. abaculum* was described by Davey (1979b) from a Barremian succession from the northern North Sea. In his study, Davey mentioned that abundant *O. abaculum* were found in the same sample as *Odontochitina operculata*, which has its first stratigraphic occurrence in the Barremian (e.g. Nøhr-Hansen, 1993; Bailey, 2019). The common occurrence of *O. abaculum* in the upper Hauterivian was reported in the UK and the Norwegian sectors of the North Sea Basin by Bailey (2019). Notably, Costa & Davey (1992) reported that in the UK sector of the North Sea Basin, *O. abaculum* has a stratigraphic range from the upper Hauterivian to lower Barremian. However, the post-Hauterivian–Barremian? age was suggested by these authors because they considered the *Simbirskites variabilis* ammonite zone as Barremian. Recently the FO of *O. abaculum* was recorded from the uppermost lower Barremian in NE Greenland by Nøhr-Hansen *et al.* (2019).

Spitsbergen – this study. Rare to common (<1 % and 1–30 % of the total dinocyst assemblage) occurrences of *O. abaculum* are observed from all sites spanning the Rurikfjellet Formation. However, in contrast to the North Sea and NE Greenland, in Spitsbergen the taxon appears in the Valanginian, i.e. much earlier than in the two other regions (Fig. 7). We consider the FO of *O. abaculum* as an intra-late Valanginian event. The diachroneity in the event (Fig. 7) would suggest that the appearance of *O. abaculum* is dependent on the local environmental changes.

Appendix 1h. FO of *Oligosphaeridium complex* (White, 1842) Davey & Williams, 1966

Figure 5h

The FO of *O. complex* is an important marker for the base Valanginian in the North Sea Basin and the Svedrup Basin, Arctic Canada (Davies, 1983; Costa & Davey, 1992; Duxbury, 2001; Bailey, 2019). From NE Greenland, Nøhr-Hansen *et al.* (2019) recently recorded the FO of *O. complex* from the *Peregrinus albidum* ammonite zone, which is latest Berriasian in age (or early Valanginian according to Ogg *et al.* 2016). On Andøya (Arctic Norway), the oldest record of *O. complex* is observed within beds assigned to the *Buchia inflata* – *Buchia keyserlingi* zones dated as early Valanginian (Århus *et al.* 1986).

Spitsbergen – this study. In our material the taxon is present in virtually all samples. In the oldest part of the record, the taxon is often characterized by a small central body size and very tilted, long processes. The process terminations often have a ‘palm-like’ appearance (Fig. 5h). We consider the FO of *O. complex* as a

marker for the base of the Valanginian. However, considering the recent study from NE Greenland it is possible that this event is slightly older (Nøhr-Hansen et al. 2019).

Appendix 1i. LO of *Palaecysta palmula* (Davey, 1982) Williams & Fensome, 2016

Figure 5k

In the UK sector of the Central North Sea Basin, the LO of *P. palmula* is observed in the middle lower Valanginian (Duxbury, 2001; Bailey, 2019), while in the Danish sector, the LO is probably slightly younger, within the lower upper Valanginian (Davey, 1982; Heilmann-Clausen, 1987) (Fig. 7).

Spitsbergen – this study. In the present study, *P. palmula* is observed in the basal part of the Rurikfjellet Formation in the Myklegardfjellet outcrop section.

Appendix 1j. Stratigraphic range of *Pseudoceratium anaphrissum* (Sarjeant, 1966) Bint, 1986

Figure 5m–o

The taxon has a remarkably short range, limited to the Barremian, primarily to the lower Barremian (Fig. 7). In the high Arctic the taxon has also been observed in the Hauterivian (Fig. 7). The Barremian record of *P. anaphrissum* is very well known from the Barents Sea (Århus et al. 1990), Arctic Norway (Thusu, 1978), offshore south Norway (Costa, 1981), NE Greenland (Nøhr-Hansen, 1993), England (e.g. Sarjeant, 1966; Duxbury, 1980), Germany (Prössl, 1990) and the North Sea Basin (Heilmann-Clausen, 1987; Costa & Davey, 1992; Bailey, 2019). Notably, in Arctic Norway a common occurrence of *P. anaphrissum* was found in a sample referred to the upper Hauterivian – lower Barremian (Århus et al. 1986). In NE Greenland, and possibly also in the UK and the Norwegian sector of the North Sea Basin, the species is abundant in a narrow interval in the middle part of its range (Nøhr-Hansen, 1993; Bailey, 2019); see also summary in Figure 7.

Spitsbergen – this study. In the present study, *P. anaphrissum* is present in the uppermost part of the Rurikfjellet Formation (Ullaberget) and the Helvetiafjellet Formation (DH2 and Ullaberget). The taxon is rare (< 1%), badly preserved and incomplete (Fig. 5m–o). All observed specimens have clearly visible antapical lobes and lateral bulges, and with no operculum. Specimens observed in DH2 and Ullaberget are covered by short spines and processes (Fig. 5n, o). Owing to a poor preservational state, the ornamentation of the specimen observed in the topmost sample from the Bohemanflya outcrop section (Fig. 5m) is difficult to establish and therefore the specimen is questionably referred to *P. anaphrissum*.

In the middle and upper part of the Rurikfjellet Formation we found the common occurrence of dinocysts which we referred to *Circulodinium distinctum* (Fig. 3g, i). The ornamentation may resemble *P. anaphrissum*, but the outline is more typical for the genus *Circulodinium*.

Appendix 1k. LO of *Sirmiodinium grossii* Alberti, 1961

Figure 6e, f

In most of the study from the North Sea Basin the LO of *S. grossii* marks the top of the Barremian (e.g. Bailey, 2019). In NE Greenland the youngest record of the taxon is observed within the lowermost Aptian (Nøhr-Hansen, 1993). More details concerning the distribution of the taxon in the Boreal and the European Boreal Realm is shown in Figure 7.

Spitsbergen – this study. We observe *S. grossii* in both the Rurikfjellet and Helvetiafjellet formations. The taxon is present in virtually all samples analysed in this study.

Appendix 1l. FO of *Subtilisphaera perlucida* (Alberti, 1959) Jain & Millepie, 1973

Figure 6g

The majority of existing records from the Boreal and European Boreal Realm suggest that *S. perlucida* appeared in the early Barremian (e.g. Heilmann-Clausen, 1987; Nøhr-Hansen, 1993). In the DH1 core the FO of *S. perlucida* was observed within the Helvetiafjellet Formation and dated as Barremian – Aptian (Midtkandal et al. 2016). Some records suggest, however, that the taxon appeared in the late Hauterivian (Fig. 7).

Spitsbergen – this study. The taxon is observed in the uppermost part of the Rurikfjellet Formation (Ullaberget) and occurs consistently in the Helvetiafjellet Formation (Ullaberget and the DH2 core).

Appendix 1m. LO of *Tubotuberella apatela* (Cookson & Eisenack, 1960) Ioannides et al. 1977

Figure 6i–k

In the majority of studies on the North Sea, the LO of *T. apatela* occurs approximately within the middle lower Valanginian (Fig. 7) and is considered synchronous with (Bailey, 2019) or slightly younger than (Duxbury, 2001) the LO of *P. palmula*. In the Barents Sea, *T. apatela* was not observed in the post-Ryazanian strata, but this may be biased by the fact that the Valanginian succession is devoid of palynomorphs (Århus et al. 1990). Numerous studies report *T. apatela* from the upper Valanginian (Davies, 1983; Århus, 1988) or even Hauterivian (Piasecki, 1979; Davey, 1982; Heilmann-Clausen, 1987) deposits. These studies report that the last persistent occurrence of *T. apatela* occurs within the lower Valanginian. In Spitsbergen and NE Greenland the post-Valanginian occurrence of the taxon is considered as reworked (Århus, 1988; Nøhr-Hansen, 1993).

Spitsbergen – this study. In the present study *T. apatela* is present within the lower to middle part of the Rurikfjellet Formation. We observe that the LO on Spitsbergen is diachronous. In the Myklegardfjellet outcrop section we apply the LO of persistent *T. apatela* as the marker for the top of the lower Valanginian (Fig. 8). *T. apatela*, in contrast to *Tubotuberella rhombiformis*, has a distinctive apical horn (on both epitheca and hypotheca) and lacks tabulation. These two features are clearly visible in virtually all specimens observed in this study.